

RESPONSES TO REVIEWERS' COMMENTS

Dear ACP Editorial Board,

We are submitting our revised paper entitled “Contrasting ambient fine particles hygroscopicity derived by HTDMA and HR-AMS measurements between summer and winter in urban Beijing.” We are grateful to the two reviewers for their insightful and constructive comments and have revised our paper accordingly to account for the reviewers’ recommendations. Below please find our detailed point-by-point responses (in blue) to the reviewers’ comments (in black) to the manuscript. We believe that we have satisfactorily addressed all criticisms from the two reviewers.

Thank you for your attention to this matter.

Sincerely, Fang Zhang on behalf of all authors

Anonymous Referee #1

Zhang et al. present a study comparing water uptake and predicted water uptake of aerosols in Beijing and North China. The authors have addressed reviewer comments and present a revised manuscript that is considerably clearer to read. I recommend publication once the following comments are addressed:

(1) Novelty

The novelty of the study could be improved. Mei et al. (2013), Zhang et al. (2016) and Zhang et al. (2017) have compared kappa derived from composition measurements to kappa measured by co-located instruments. Mei et al. (2013) derive an empirical relationship between f44 and kappa_{org} based on their observations. This relationship may not apply to dissimilar field sites. The correlation between f44 or O:C ratio and kappa is not always linear. The correlation between oxidation and kappa is strong but nevertheless an empirical relationship resulting from underlying molecular composition. Zhang et al. (2016), Zhang et al. (2017), and the current study discuss over- and under-prediction of kappa for their measurements. I think it is generally acknowledged that different emission profiles result in different chemistry – I recommend discussing these differences, and perhaps

de-emphasizing the poor representation of the measurement by published empirical models. This model/measurement disagreement has already been discussed (Zhang et al., 2016, Zhang et al., 2017).

Re: we appreciate the comments. We have revised the corresponding discussions in the paper as follows (or lines 377-392),

“...The uncertainty in calculation of κ_{chem} may be also related to the uncertainty caused by composition of organics that vary widely over a range of diverse constituents of SOA (Suda et al., 2012). The lower κ_{chem} indicates that the κ of secondary organic aerosols formed through the strong photochemical oxidation processes in summer of urban Beijing are likely underestimated. In this study, the mean κ value of organics derived from the f_{44} parametrized equation is 0.20 ± 0.02 , ranging from 0.17 to 0.23 during 09:00-17:00. While the organic aerosols, especially for particles in accumulated mode, may be more hydrophilic with much larger κ , i.e. >0.2 due to large formation of highly-oxidized OA. One can easily get that increasing the κ of organic aerosols from 0.2 to 0.3 can explain about 11-13% underestimation of κ_{chem} , but representing an upper limit of the impact of hygroscopicity of organic aerosols on the calculation. This is because that the κ value of 0.3 corresponds to the maximum possible for ambient organic aerosols. Additionally, the f_{44} parametrized equation tends to overestimate the κ according to Fröhlich et al. (2015), which should yield a larger κ_{chem} . Finally, the coexisting hygroscopic and hydrophobic species may have a strong influence on the phase state of particles, also likely affecting chemical interactions between inorganic and organic compounds as well as the overall hygroscopicity of mixed particles (Peng et al., 2016). Overall, The lower κ_{chem} caused by the photochemical aging effect is likely resulted from multiple impacts of inappropriate application of density and hygroscopic parameter of organic aerosols in the calculation, as well as the influences from chemical interaction between organic and inorganic compounds on the overall hygroscopicity of mixed particles. This topic warrants further investigations.”

(2) Coating effect

I think that the coating effect on hygroscopicity should be discussed with appropriate caveats. I find it unlikely that a coating of organic material on an inorganic core limits uptake of water as implied. Studies have shown that water diffusion into viscous organics is fast. These rates are published and will show that for nanoscale aerosol, it is unlikely that condensing SOA prevents water uptake by an inorganic core. Various other quantities go into κ_{chem} , including e.g. density as the other reviewer has mentioned and also composition (and hygroscopicity) of the organic. These are good candidates for the underlying mechanisms causing poor agreement between model and measurement.

Re: Thanks a lot for the comments. We agree with that to address the coating effect with appropriate caveats. We have revised the corresponding discussions and statements in the paper (see revised Abstract, Section 3.4 and Conclusions). Specifically, previous statements about coating effect have been presented as “aging effect”. We have provided revised statements of following to explain the lower κ_{chem} around noontime in summer,

“The lower κ_{chem} caused by the photochemical aging effect is likely resulted from multiple impacts of inappropriate application of density and hygroscopic parameter of organic aerosols in the calculation, as well as the unknown influences from chemical interaction between organic and inorganic compounds on the overall hygroscopicity of mixed particles.”

(3) Technical corrections

The manuscript would benefit from a careful reading to correct technical errors. Two examples are included here, but there are many more.

Re: Careful corrections of technical errors throughout the manuscript have been done.

Lines 27-28: This sentence needs reworking. "the hypothesis" is mentioned before it is defined.

Re: Revised.

Line 29: on average

Re: Revised.

(4) References:

Mei, F., Setyan, A., Zhang, Q., and Wang, J.: CCN activity of organic aerosols observed downwind of urban emissions during CARES, *Atmos. Chem. Phys.*, 13, 12155–12169, <https://doi.org/10.5194/acp-13-12155-2013>, 2013.

Zhang, F., Wang, Y., Peng, J., Ren, J., Collins, D., Zhang, R.,...Li, Z. (2017). Uncertainty in predicting CCN activity of aged and primary aerosols. *Journal of Geophysical Research: Atmospheres*, 122. <https://doi.org/10.1002/2017JD027058>

Zhang, F., Li, Z., Li, Y., Sun, Y., Wang, Z., Li, P., Sun, L., Wang, P., Cribb, M., Zhao, C., Fan, T., Yang, X., and Wang, Q.: Impacts of organic aerosols and its oxidation level on CCN activity from measurement at a suburban site in China, *Atmos. Chem. Phys.*, 16, 5413–5425, <https://doi.org/10.5194/acp-16-5413-2016>, 2016.

Anonymous Referee #2

This revised manuscript has addressed all my previous concerns. Meanwhile, the further discovery that an inappropriate use of BC density may cause significant overestimation of the hygroscopic parameter, is really intriguing, making the current version much better in terms of scientific novelty. I suggest the publication of this manuscript in ACP after a minor revision. The disparity between k_{chem} and k_{gf} during rush hour could also be attributed to the bias from the HTDMA measurements. The HTDMA may overestimate the D_{dry} for the external mixed fractal BC particles, as BC-containing particles may shrink when humidified, leading to underestimate the hygroscopic growth factor.

Re: We have included a statement to address the uncertainty caused by the HTDMA techniques in the revised version (see lines 273-275).

The language and expression need to be improved. Some examples are listed as follows.

Re: Careful corrections of technical errors throughout the manuscript have been done.

Line 57, the sentence could be revised as "In a heavily polluted atmosphere with varied aerosol sources and sinks as well as complex physical and chemical processes, the mixing state and its impact on aerosols hygroscopicity is more complicated."

Re: Revised.

Line 61, this is not a complete sentence.

Re: Corrected and Revised.

Line 69, "during the periods dominated by primary emissions"

Re: Revised.

Line 76, "has been lacking" is really a weird expression.

Re: Revised as "A comprehensive investigation on the causes and magnitude of the effect is with great significance to parameterize the effect of atmospheric processes/emissions of aerosols on particles hygroscopicity in models."

Line 83, this sentence is weird, try revising it.

Re: Revised.

Line 289, change "which" to "it".

Re: Corrected.

Line 302, delete "and"

Re: Deleted.

1 **Contrasting ambientsize-resolved hygroscopicity of fine particles ~~hygroscopicity~~ derived by HTDMA**
2 **and HR-AMS measurements between summer and winter in urban Beijing: the impacts of aerosol**
3 **aging and local emissions on its hygroscopicity**

4 Xinxin Fan^{1,*}, Jieyao Liu^{1,*}, Fang Zhang^{1,‡,#}, Lu Chen¹, Don Collins², Weiqi Xu^{3,4}, Xiaoi Jin¹, Jingye
5 Ren¹, Yuying Wang^{1,5}, Hao Wu¹, Shangze Li¹, Yele Sun^{3,4}, Zhanqing Li^{1,6}

6
7 ¹State Key Laboratory of Earth Surface Processes and Resource Ecology, College of Global Change and
8 Earth System Science, Beijing Normal University, Beijing 100875, China

9 ²Department of Chemical and Environmental Engineering, University of California Riverside, Riverside,
10 California, USA

11 ³State Key Laboratory of Atmospheric Boundary Layer Physics and Atmospheric Chemistry, Institute of
12 Atmospheric Physics, Chinese Academy of Sciences, Beijing 100029, China

13 ⁴College of Earth Sciences, University of Chinese Academy of Sciences, Beijing 100049, China

14 ⁵School of Atmospheric Physics, Nanjing University of Information Science and Technology, Nanjing
15 210044, China

16 ⁶Earth System Science Interdisciplinary Center and Department of Atmospheric and Oceanic Science,
17 University of Maryland, College Park, Maryland, USA

18
19 *Those authors contribute equally to this work

20
21 #Correspondence to: Fang.zhang@bnu.edu.cn

22 **Abstract**

23 The effects of aerosols on visibility through scattering and absorption of light and on climate through
24 altering cloud droplet concentration are closely associated with their hygroscopic properties. Here, based on
25 field campaigns in winter and summer in Beijing, we compare the size-resolved hygroscopic parameter (κ_{gf})
26 of ambient fine particles derived by an HTDMA (Hygroscopic Tandem Differential Mobility Analyzer) to
27 that (denoted as κ_{chem}) of calculated by an HR-ToF-AMS (High-resolution Time-of-Flight Aerosol Mass
28 Spectrometer) measurements using a simple rule with athe hypothesis of uniform internal mixing
29 hypothesisof aerosol particles. We mainly focus on contrasting the disparity of κ_{gf} and κ_{chem} between summer
30 and winter to reveal the impact of atmospheric processes/emission sources on aerosols hygroscopicity and to
31 evaluate the uncertainty in estimating particles hygroscopicity with the hypothesis. We show that, in summer,
32 the κ_{chem} for 110, 150 and 200 nm particles was averagelyon average ~10% - 12% lower than κ_{gf} , with the

greatest difference between the values observed around noontime when aerosols experience rapid photochemical aging. In winter, no apparent disparity between κ_{chem} and κ_{gf} is observed for those >100 nm particles around noontime, but the κ_{chem} is much higher than κ_{gf} in the late afternoon when ambient aerosols are greatly influenced by local traffic and cooking sources. By comparing with the observation from other two sites (Xingtai, Hebei and Xinzhou, Shanxi) of north China, we verify that atmospheric photochemical aging of aerosols enhances their hygroscopicity and ~~may induce a coating effect which thereby~~ leads to 10%-20% underestimation ~~of the hygroscopic parameter in κ_{chem}~~ if using the uniform internal mixing assumption. The ~~coating~~ effect is found more significant for these >100 nm particles observed in remote or clean regions. ~~However~~The lower κ_{chem} is likely resulted from multiple impacts of inappropriate application of density and hygroscopic parameter of organic aerosols in the calculation, as well as influences from chemical interaction between organic and inorganic compounds on the overall hygroscopicity of mixed particles. We also find that, local/regional primary ~~sources~~emissions, which result in a large number of externally-mixed BC and POA (Primary Organic Aerosol) in urban Beijing during traffic rush hour time, cause 20-40% overestimation of the hygroscopic parameter. This is largely due to an inappropriate use of density of the BC particles that is closely associated with its morphology, ~~and the or degree of its aging. The~~ results show that the calculation can be improved by applying an effective density of freshly BC ~~within the range of (0.25-0.45 g cm⁻³)~~ in the mixing rule assumption. Our study suggest that it is critical to measure the effective density and morphology of ambient BC in ~~particularity~~particularly in those regions with ~~complex~~influences of rapid secondary conversion/aging processes and local sources, so as to accurately parameterize the effect of BC aging on particles hygroscopicity.

1. Introduction

The effects of aerosols on visibility through scattering and absorption of light and on climate through altering cloud droplet concentration are influenced by their hygroscopic growth. Understanding and reducing the uncertainty in prediction of the aerosol hygroscopic parameter (κ) using chemical composition would improve model predictions of aerosol effects on clouds and climate.

58 The hygroscopic properties of both the natural and anthropogenic aerosols, in addition to being affected
59 by its chemical composition (Gunthe et al., 2009), are also affected by the particle mixing state and aging
60 (Schill et al., 2015; Peng et al., ~~2017~~2017a). For example, a recent laboratory study ~~shown~~showed that the
61 coexisting hygroscopic species have a strong influence on the phase state of particles, thus affecting
62 chemical interactions between inorganic and organic compounds as well as the overall hygroscopicity of
63 mixed particles (Peng et al., ~~2016~~2016a). The field measurements also demonstrated that the hydrophobic
64 black carbon particles became hygroscopic with atmospheric mixing and aging by organics (i.e. Peng et al.,
65 ~~2017~~2017a). In a heavily polluted atmosphere, ~~the with varied~~ aerosol sources and sinks ~~are varied, the as~~
66 ~~well as complex~~ physical and chemical processes ~~experienced by the aerosols are complex, and,~~ the mixing
67 state and its impact on aerosols ~~hygroscopicity is more complicated.~~ The hygroscopicity of mixed particles
68 and mutual impacts between the components are still poorly understood.

带格式的

带格式的: 字体: Times New Roman,

69 Previous studies have shown that the difference between the κ obtained from H-TDMA or CCNc
70 measurements and ~~that~~ calculated based on the volume mixing ratio of chemical components, ~~κ_{chem}~~ .
71 Laboratory results from Cruz and Pandis (2000) indicate that κ_{gf} of internally mixed ammonium sulfate and
72 organic matter is higher than κ_{chem} calculated for assumed uniform internal mixing. But Peng et al
73 (~~2016~~2016a) found that, for sodium chloride and organic aerosols mixed particles, the measured growth
74 factors by H-TDMA were ~~significantly~~ lower than calculations from the mixing rule methods. In some field
75 studies on aged aerosols, the κ was underestimated by the calculation based on uniform internal mixing
76 assumption and thus lead to an underestimation of CCN concentration (Bougiatioti, et al., 2009; Chang, et al.,
77 2007; Kuwata, et al., 2008; Wang, et al., 2010; Ren et al., 2018). However, ~~for~~during primary
78 ~~emission~~emission dominated periods, the κ value from calculations based on bulk chemical composition
79 was much higher than that measured by H-TDMA measurements (Zhang et al., 2017). The various results
80 from previous studies suggest distinct effects of aerosols mixing state on their hygroscopicity. Overall, to
81 what extent do the differences depend on the mixing state and the extent of aging of the particles, and how
82 the different atmospheric processes and what kinds of mixing structure of the particles may result in those
83 disparity between measured and calculated hygroscopic parameter have not been clearly clarified by the

带格式的: 字体: Times New Roman

84 previous studies. ~~A comprehensive and systematic~~ investigation on the ~~cause~~causes and magnitude of the
85 effect ~~has been lacking~~is with great significance to parameterize the effect of atmospheric
86 ~~processes/emissions of aerosols on particles~~hygroscopicity in models.

87 In the atmosphere, the κ , which is related to the particle mixing state diversity, varies largely across
88 the size range of ambient fine particles (Rose et al., 2010). ~~Previous~~However, ~~previous~~ study ~~only just~~
89 compared the ~~measured~~ κ ~~to that~~ calculated ~~based on~~from bulk chemical composition ~~to that measured by~~
90 ~~H-TDMA~~ (Zhang et al., 2017). Using size-resolved, not bulk, chemical composition measurements in
91 different seasons, is expected to provide more comprehensive understanding and insights of how the
92 aerosols mixing state influence on their hygroscopicity, motivating our analysis that employs size-resolved
93 chemical composition measured by an HR-ToF-AMS in this study. The aim of this paper is to study the
94 hygroscopicity and mixing state characteristics of fine particles in the Beijing urban area, and to reveal the
95 impact of atmospheric processes/sources and mixing/aging on aerosols hygroscopicity and elucidate the
96 uncertainty in calculating the hygroscopic parameter using simple mixing rule estimates based on
97 size-resolved chemical composition. The experiment and theory in the study are introduced in Sect. 2. The
98 comparison between the hygroscopic parameter obtained from the HTDMA and and that calculated using
99 size-resolved chemical composition is discussed in Sect. 3. Conclusions from the study are given in Sect. 4.

100 2. Experiment and Theory

101 2.1. Site and instruments

102 Two field campaigns are conducted during winter 2016 and summer 2017 of urban Beijing (Fig. 1, BJ:
103 39.97°N, 116.37°E) for measurements of aerosols physical and chemical properties. The BJ site is located
104 at the Institute of Atmospheric Physics (IAP), Chinese Academy of Sciences, which is between the north
105 third and fourth ring roads in northern Beijing. Local traffic and cooking emissions can be important at the
106 site (Sun et al., 2015). The sampling period in cold season was from 16 November to 10 December 2016,

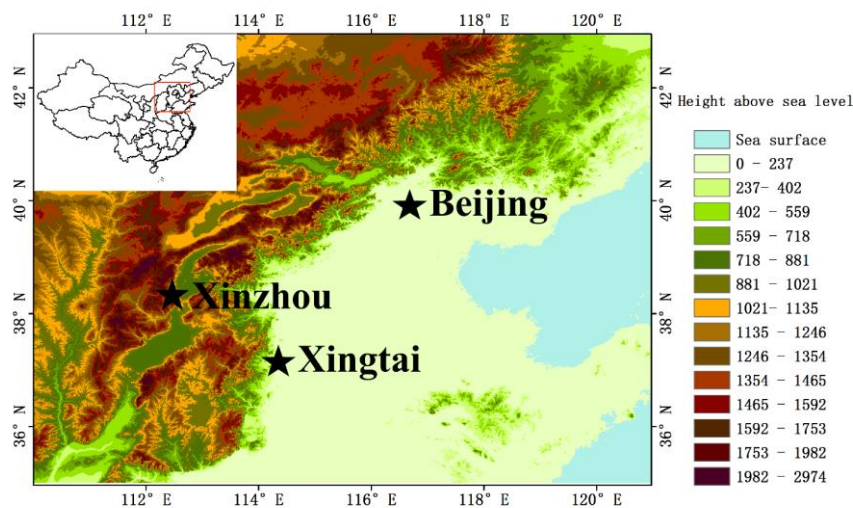
带格式的: 字体: 倾斜

带格式的: 字体: 倾斜

带格式的: 字体: 倾斜

带格式的: 字体: 倾斜

107 during the domestic heating period in Beijing. The sampling period in warm season was from 25 May to 18
108 June 2017.



109
110 Figure 1. The map location of the sites
111

112 Particle number size distribution (PNSD) in the size range from 10 nm to 550 nm was measured with a
113 Scanning Mobility Particle Sizer (SMPS; Wang & Flagan, 1990; Collins et al., 2002), which consists of a
114 long differential mobility analyzer (DMA, model 3081L, TSI Inc) to classify the particle and a condensation
115 particle counter (CPC, model 3772, TSI Inc.) to detect the size classified particles. The sampled particles
116 were dried to relative humidity < 30% before entering the DMA. The measurement time for each size
117 distribution was five minutes.

118 The HTDMA system used in this study has been described in detail in previous publications (Tan et al.,
119 2013; Wang et al., 2017; Zhang et al., 2017). Here, only a brief description is given. A Nafion dryer dried
120 the sampled particles to relative humidity < 20%, after which the steady state charge distribution was
121 reached in a bipolar neutralizer. The first differential mobility analyzer (DMA₁, model 3081L, TSI Inc.)
122 selected the quasi-monodisperse particles through applying a fixed voltage. The dry diameters selected in
123 this study were 40, 80, 110, 150, and 200 nm. The quasi-monodisperse particles were humidified to a

124 controlled RH (90% in this study) using a Nafion humidifier. A second DMA (DMA₂, same model as the
125 DMA₁) coupled with a water-based condensation particle counter (WCPC, model 3787, TSI Inc.) measured
126 the particle number size distributions of the humidified aerosol. RH calibration with ammonium sulfate was
127 carried out regularly during the study.

128 The hygroscopic growth factor (Gf) is defined as the ratio of the mobility diameter at a given RH to the
129 dry diameter:

$$Gf = \frac{D(RH)}{D(dry)}$$

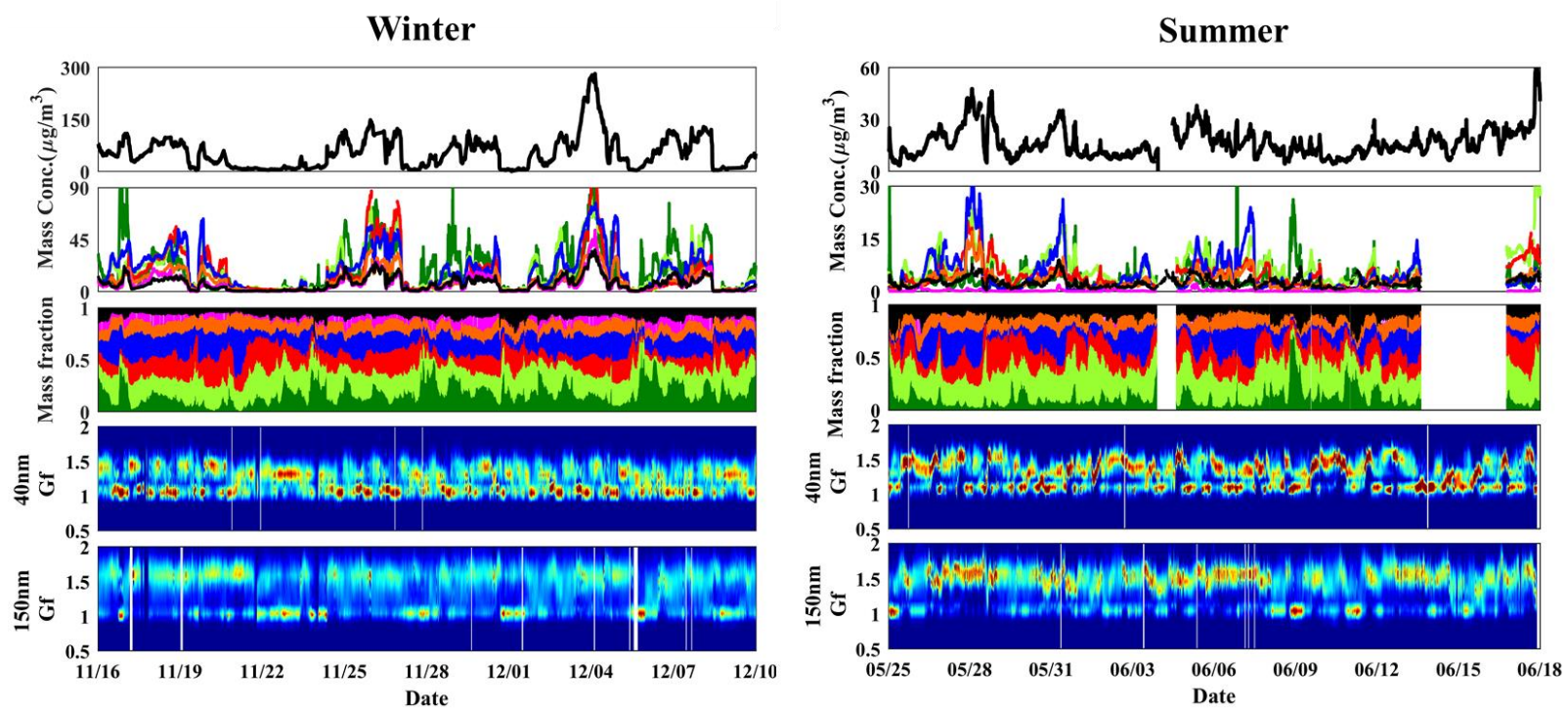
130 The Gf probability density function (PDF) is retrieved based on the TDMA_{inv} algorithm developed by
131 Gysel et al. (2009). Dry scans in which the RH between the two DMAs was not increased were used to
132 define the width of the transfer function.

133 Size-resolved non-refractory submicron aerosol composition was measured with an Aerodyne
134 high-resolution time-of-flight aerosol mass spectrometer (HR-ToF-AMS; Xu et al., 2015). The particle
135 mobility diameter was estimated by dividing the vacuum aerodynamic diameter from the AMS
136 measurements by particle density. Because the uncertainty caused by the fixed density across the size range
137 is negligible (Wang et al. 2016), here, the particle density is assumed to be 1600 kg m⁻³ (Hu et al., 2012).
138 AMS positive matrix factorization (PMF) with the PMF2.exe (v4.2) method was performed to identify
139 various factors of organic aerosols. Xu et al. (2015) have described the operation and calibration of the
140 HR-ToF-AMS in detail. Black carbon (BC) mass concentration was derived from measurements of light
141 absorption with a 7-wavelength aethalometer (AE33, Magee Scientific Corp.; Zhao et al., 2017).

142 **2.2. Data**

143 The time series of the submicron particle mass concentration PM₁, bulk mass concentrations of the
144 main species in PM₁, mass fraction of the chemical composition of PM₁, and probability density function of
145 growth factor (Gf-PDFs) for 40 and 150 nm particles during the campaign are presented in Fig. 2. Quite
146 distinct temporal variability of aerosol chemical and physical properties was observed between winter and

147 summer. The average mass concentration of PM_{10} was $55.2 \mu\text{g}/\text{m}^3$ in the winter and $16.5 \mu\text{g}/\text{m}^3$ in the
148 summer during our study periods. In this study, we define the conditions when the mass concentration in
149 winter period was $< 20 \mu\text{g m}^{-3}$ and $>80 \mu\text{g m}^{-3}$ as clean and polluted conditions, respectively. Organic
150 aerosol (OA), consisting of secondary organic aerosol (SOA) and primary organic aerosol (POA), was the
151 major fraction during both the winter and summer sampling periods. POA concentration was higher than
152 that of SOA in the winter, which reflects the influence of primary emissions such as coal combustion OA
153 (COOA) in Beijing (Hu et al., 2016; Sun et al., 2016). In contrast, SOA usually dominated in the summer,
154 which is evident that secondary aerosol formation played a key role in the source of PM_{10} . Distinct
155 hydrophobic (with Gf of ~ 1.0) and more hygroscopic (with Gf of ~ 1.5) modes were observed from Gf-PDFs
156 of both small and large particles. Sometimes the more hygroscopic mode particles were more concentrated
157 and at others the hydrophobic particles were. In general though, the more hygroscopic mode dominated for
158 larger particles (i.e. 150 nm), and the less hygroscopic mode did for the smallest particles (e.g. 40 nm).
159 Occasionally, only the hydrophobic mode was evident for 150 nm particles, which occurred when POA
160 dominated the PM_{10} . Only the hygroscopic mode was discernable for 40 nm particles during new particle
161 formation (NPF) events that occurred more frequently in summer than winter (Fig. 3).



162

163

Figure 2. Winter (left) and summer (right) time series of mass concentration of PM_{10} , bulk mass concentration of the main species in PM_{10} , mass fraction

164

of the chemical composition of PM_{10} and Gf-PDFs for 40 and 150 nm particles.

2.3. Theory and method

2.3.1 Derivation of the hygroscopic parameter, κ , from the growth factor (Gf)

According to κ -Köhler Theory (Petters and Kreidenweis, 2007), the hygroscopicity parameter κ can be derived using the growth factor measured by an HTDMA.

$$\kappa = (Gf^3 - 1) \left(\frac{\exp\left(\frac{A}{D_d Gf}\right)}{RH} - 1 \right), \quad (1)$$

$$A = \frac{4\sigma_{s/a} M_w}{RT \rho_w}, \quad (2)$$

where Gf is hygroscopic growth factor measured by HTDMA, D_d is the dry diameter of the particles, RH is the relative humidity in the HTDMA (90%, in our study), $\sigma_{s/a}$ is the surface tension of the solution/air (assumed here to be the surface tension of pure water, $\sigma_{s/a} = 0.0728 \text{ N m}^{-2}$), M_w is the molecular weight of water, R is the universal gas constant, T is the absolute temperature, and ρ_w is the density of water.

2.3.2 Derivation of the hygroscopic parameter, κ , from chemical composition data

For an assumed internal mixture, κ can also be calculated by a simple mixing rule on the basis of chemical volume fractions (Petters and Kreidenweis, 2007; Gunthe et al., 2009):

$$\kappa_{chem} = \sum_i \varepsilon_i \kappa_i, \quad (3)$$

where κ_i and ε_i are the hygroscopicity parameter and volume fraction for the individual (dry) component in the mixture, respectively. The AMS provides mass concentrations of organics and of many inorganic ions. The inorganic components mainly consisted of $(\text{NH}_4)_2\text{SO}_4$ and NH_4NO_3 (Zhang et al., 2014). And the values of κ are 0.48 for $(\text{NH}_4)_2\text{SO}_4$ and 0.58 for NH_4NO_3 (Petters and Kreidenweis, 2007). To estimate κ_{org} , we used the following linear function derived by Mei et al. (2013): $\kappa_{\text{org}} = 2.10 \times f_{44} - 0.11$. We derived the

184 volume fraction of each species by dividing mass concentration by its density. The density are 1.77 g cm^{-3}
185 for $(\text{NH}_4)_2\text{SO}_4$ and 1.72 g cm^{-3} for NH_4NO_3 . The densities of organics are assumed to be 1.2 g cm^{-3} (Turpin
186 et al., 2001). The κ and density of BC are assumed to be 0 and 1.7 g cm^{-3} . In the following discussions, κ_{gf}
187 and κ_{chem} denote the values derived from HTDMA measurements and calculated using the ZSR mixing rule,
188 respectively.

189 In addition, we also compare the results from the field campaigns with those from other two sites,
190 Xingtai (XT: 37.18°N , 114.37°E), and Xinzhou (XZ: 38.24°N , 112.43°E), in North China Plain (Fig. 1).
191 At XZ site, we use the hygroscopic parameter (defined as κ_{CCNc}) from size-resolved CCN measurements
192 (Zhang et al., 2014, 2016) for comparison. More detailed descriptions of the method to retrieve κ_{CCNc} can be
193 found in (Petters and Kreidenweis (2007)). Both of the κ_{gf} and κ_{CCNc} are derived based on κ -Köhler Theory
194 (Petters and Kreidenweis, 2007). But, different from the κ_{gf} measured by the HTDMA system which is
195 operated at RH of 90%, the κ_{CCNc} is derived by measuring aerosols CCN activity under the condition of
196 supersaturations with relative humidity of $>100\%$. Previous studies from filed measurements and laboratory
197 experiments showed that the κ_{CCNc} is generally slight larger or smaller than κ_{gf} , but they are basically
198 comparable and can well represent an overall aerosols hygroscopicity (e.g. Carrico et al., 2008; Wex et al.,
199 2009; Good et al., 2010; Irwin et al., 2010; Cerully et al., 2011; Wu et al., 2013; Zhang et al., 2017).

200 **3. Results and discussion**

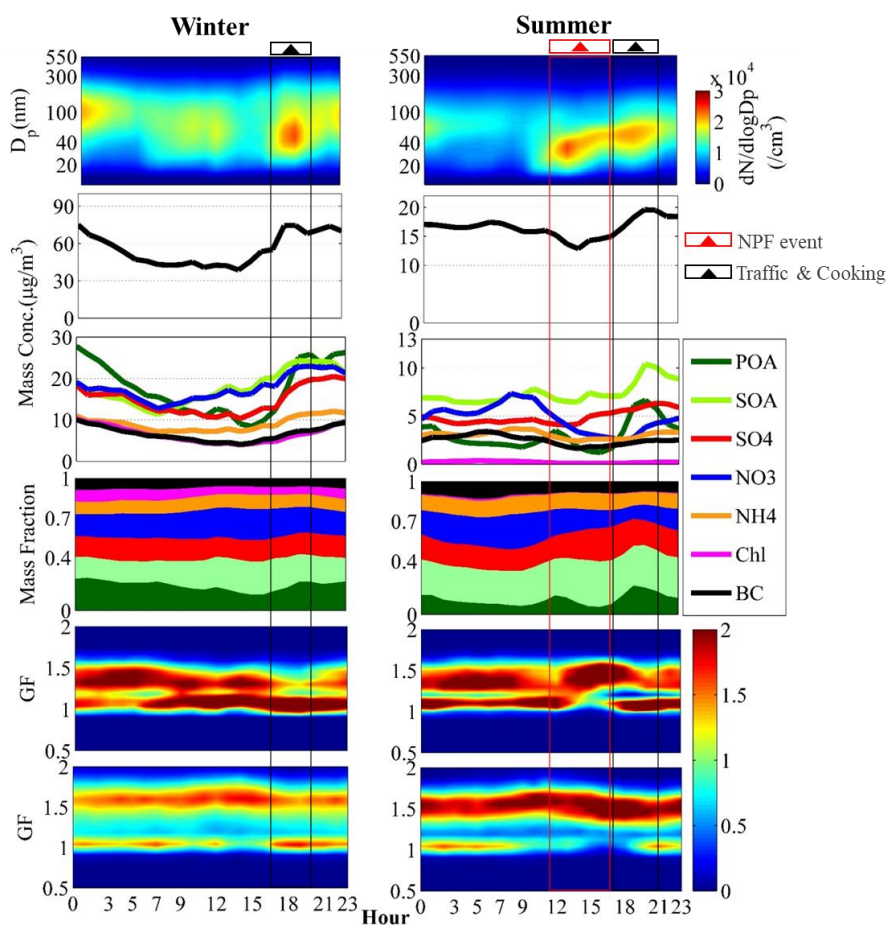
201 **3.1. Diurnal variations of ambient fine particles physiochemical properties and hygroscopic growth** 202 **factor**

203 The diurnal variations of the PNSD, mass concentration of PM_{10} , mass concentration and fraction of
204 chemical components in PM_{10} , and Gf-PDFs for 40 and 150 nm particles during the campaign are shown in
205 Fig. 3. During the summer an obvious peak value in the PNSD is observed around noontime due to NPF
206 events that typically started around 10:00 LT (Local Time). The resulting sharp increase in number

207 concentration of nucleation mode particles was followed by decreased concentration and a rapid growth in
208 diameter of the particles along with increased mass concentration of SOA and sulfate in PM₁, indicating
209 strong photochemical and secondary formation processes during daytime in the summer ([Peng et al., 2017b](#),
210 Marked in red box in Fig. 3). In contrast, NPF was not evident during the winter period, which may in part
211 be due to the much higher (~3x) PM₁ mass concentrations in the winter than in the summer. Note that peak
212 values in number concentration and in mass concentrations of PM₁ and POA occurred during the early
213 evening (17:00-21:00, LT) indicating the strong impact of local sources from traffic emissions and cooking
214 (Marked in black box in Fig. 3, [Peng et al., 2014](#)). In addition, the diurnal cycles of aerosol physical and
215 chemical properties are also influenced by the diurnal changes in the planetary boundary layer (PBL) that
216 leads to accumulation of particles during nighttime when higher values of both number and mass
217 concentration were observed.

218 Owing to the continued local and primary emissions near the study site, the Gf-PDFs for 40 nm
219 particles generally display a bimodal shape with more and less hygroscopic modes (with Gf of ~ 1.5 and ~
220 1.1 respectively) throughout the day both in winter and summer periods, indicating an external mixing state
221 for the 40 nm particles. Note that, during nighttime and early morning in the winter, the more hygroscopic
222 mode dominated and was shifted to higher Gf than during the daytime. This is thought to be due to
223 heterogeneous/aqueous reactions on pre-existing primary small particles, and/or coagulation/condensation
224 processes that are enhanced at night under lower ambient temperature and higher relative humidity, all of
225 which result in a more hygroscopic and more internally-mixed aerosol (Liu et al., 2011; Massling et al.,
226 2005; Ye et al., 2013; Wu et al., 2016; Wang et al., 2018a). Interestingly, in the summer period, the
227 concentration of the hydrophilic mode increased quickly around noontime and in the early afternoon
228 (12:00-16:00), with a corresponding decrease in the relative concentration of the hydrophobic mode, which
229 likely indicates a transformation of the particles from externally to internally mixing state as a result of the
230 species condensation from the photochemical reaction (Wu et al., 2016; Wang et al., 2017), resulting in an
231 increase in particle hygroscopicity. In addition, it is evident that 40 nm particles after 12:00 were dominated
232 by NPF (Fig. 3). Therefore, the increase of hydrophobic mode particles suggests that a large amount of

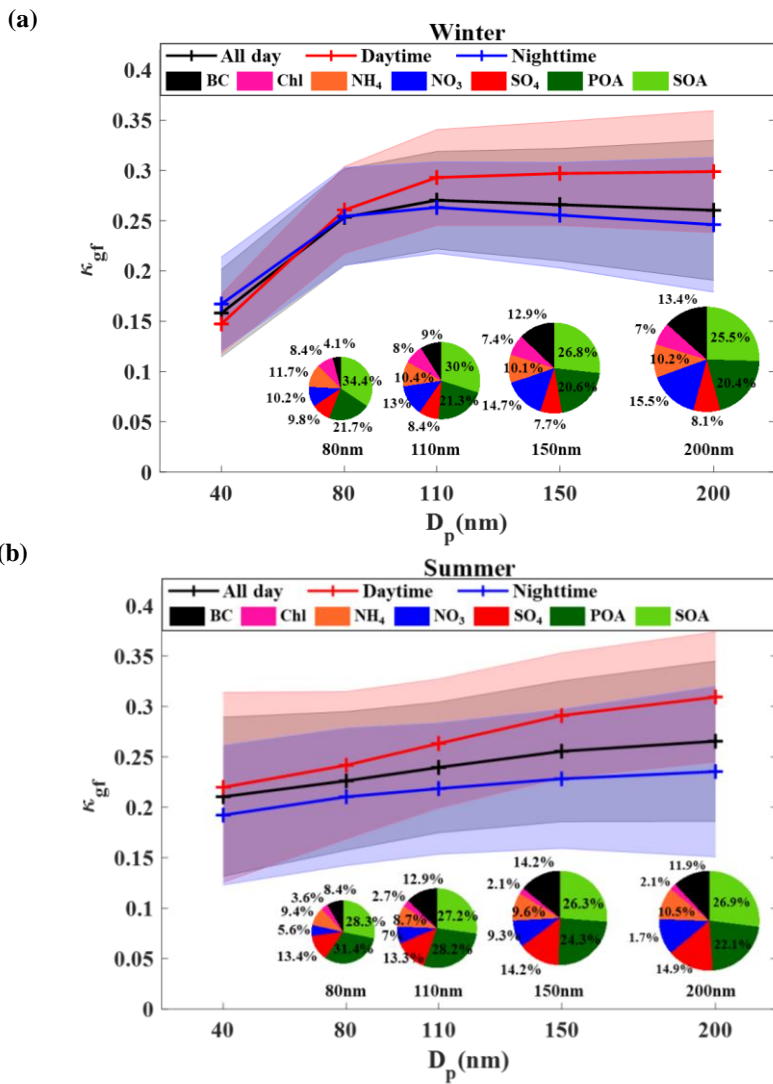
233 hydrophilic particles are generated from NPF. For 150 nm particles, the hygroscopic mode in the Gf-PDF is
 234 more dominant during daytime in particular during the summer period when the strong solar radiation
 235 promotes photochemical aging and growth, thus producing a more internally-mixed aerosol. The dominant
 236 hydrophobic mode at around 18:00 was observed both in winter and summer and reflects abundant traffic
 237 emissions and cooking sources (primarily with POA) during the early evening period.



238
 239 Figure 3. Campaign averaged diurnal variations in particle number size distribution; mass concentration of
 240 PM_{10} , bulk mass concentration of main species in PM_{10} , mass fraction of chemical composition of PM_{10} ; and
 241 Gf-PDFs for 40 and 150 nm particles in winter (left panels) and summer (right panels) measured in urban
 242 Beijing..

243 **3.2 κ_{gf} dependence on D_p**

244 The size dependence of particle hygroscopicity parameters for the winter and summer periods are
 245 presented in Fig.4. In the winter, the 40 nm particles were least hygroscopic and the hygroscopicity of larger
 246 particles (>80 nm) displayed insignificant dependence on particle size. The size independence for the larger
 247 particles is consistent with the observed similarity in mass fractions of inorganic and organic species across



250 Figure 4. The dependence of κ on D_p at the urban Beijing site during winter (a) and summer (b). The κ
251 values are retrieved from the size-resolved HTDMA measurements. The error bars represent $\pm 1\sigma$. The
252 size-resolved chemical mass fractions at the corresponding D_p is also presented.

253 the size range as shown in the pie charts in Figure 4a. A similar dependence of particle hygroscopicity on
254 particle size was also observed in the urban area of Beijing during the wintertime of 2014 (Wang et al.,
255 2018b). In the summer, hygroscopicity increased with increasing particle size, which is expected based on
256 the size dependent patterns shown in the pie charts, with the mass fraction of POA decreasing with the
257 particles size and the mass fraction of inorganics like sulfate and nitrate increasing with particle size.

258 3.3. Closure of HTDMA and chemical composition derived κ

259 A closure study was conducted between κ_{chem} and κ_{gf} (Fig. 5) to investigate the uncertainty of the two
260 methods, and especially to further illustrate whether particle hygroscopicity can be well predicted by κ_{chem}
261 calculated by assuming internal mixing. Since a size-resolved BC mass concentration measurement was not

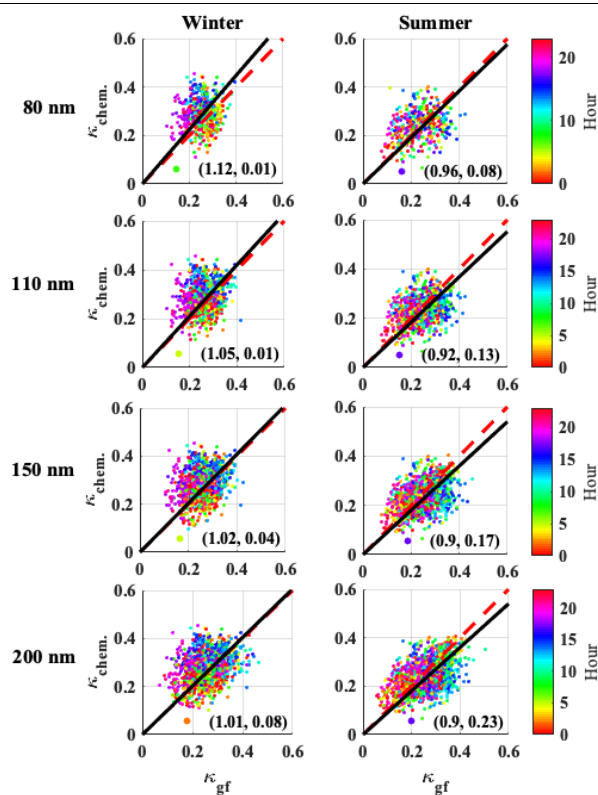


Figure 5. Closure of κ_{chem} calculated from size-resolved chemical composition data and κ_{gf} retrieved from hygroscopic growth factor by HTDMA measurements in winter (left panels) and summer (right panels) period. The dots with different color correspond to observed time of a day during the campaign as shown by the color bar. On each plot, red dotted line is 1:1 line, black solid line is fitting line. The numbers in parentheses are slopes of linear fits and correlation coefficients (R^2).

available during the campaign, we use the bulk mass fraction of BC particles measured by the AE33 combining with size-resolved BC distribution measured by a single particle soot photometer (SP2) in Beijing (Liu et al., 2018) to estimate κ_{chem} . During the calculation, the BC core diameter measured by SP2 has been converted to the diameter of coated BC particles by multiplying factors of 1.4 and 2.6 under clean (with bulk BC mass concentrations $< 2 \mu\text{g m}^{-3}$) and polluted (with bulk BC mass concentrations $> 2 \mu\text{g m}^{-3}$) conditions respectively (Liu et al., 2018).

275 Uncertainty in κ is due in part to measurement uncertainty of the HTDMA system and uncertainty
276 resulting from non-ideality effects in the solution droplets, surface tension reduction due to surface active
277 substances, and the presence of slightly soluble substances that dissolve at RH higher than that maintained in
278 the HTDMA (e.g., Wex et al., 2009; Good et al., 2010; Irwin et al., 2010; Cerully et al., 2011; Wu et al.,
279 2013). For example, the HTDMA may overestimate the D_p of dry particles for the external mixed BC
280 particles, as BC-containing particles may shrink when humidified, leading to underestimate the hygroscopic
281 growth factor. However, our previous study demonstrated that, for this region, estimates using HTDMA data
282 are still better representing the aerosols hygroscopicity than those using the simple mixing rule based on
283 chemical volume fractions for an assumed internal mixture (Zhang et al., 2017). Therefore, here we focus on
284 discussing and exploring the uncertainty of κ_{chem} by taking κ_{gf} as the reference.

285 The results show that, although the slopes from linear fitting of κ_{chem} and κ_{gf} are close to 1.0, it is with
286 quite poor correlations (typically with correlation coefficients, R^2 , of < 0.3) between κ_{chem} and κ_{gf} of the 80,
287 110, 150, 200 nm particles both in winter and summer. The poor correlations reflect large uncertainty in one
288 or both of the calculated parameters that are likely due to the unreasonable assumption of particle mixing
289 state (e.g. Cruz and Pandis, 2000; Svenningsson et al., 2006; Sjogren et al., 2007; Zardini et al., 2008),
290 which varies with their aging and other physiochemical processes in the atmosphere. Note that
291 underestimation of κ_{chem} for the summer occurred mostly in the afternoon (Marked in blue dots in Fig. 5).
292 This may be associated with photochemical processes at around noontime. More specific investigations of
293 the particle mixing and aging impacts on κ_{chem} will be further addressed in the following sections.

294 **3.4 Aerosols aging processes and sources effects indicated by diurnal cycles of κ_{chem} and κ_{gf}**

295 The diurnal cycles of particle hygroscopicity in the summer and winter with the use of the size-resolved
296 chemical composition observations and the ratio of κ_{chem} to κ_{gf} are shown in Fig. 6. In summer, at
297 09:00-15:00, the disparity between κ_{chem} and κ_{gf} is insignificant for smaller particles (80 and 110 nm), both
298 of ~~which~~them show slight decrease from 09:00 or 10:00 to 12:00-13:00 due to the frequent NPF event that
299 usually corresponds to a large fraction of organics (Fig. 3) in urban Beijing. For larger particles (150 and

带格式的: 字体颜色: 自动设置

200 nm), the disparity between κ_{chem} and κ_{gf} around noontime and in the early afternoon is very significant, corresponding to >20% underestimation of particle hygroscopicity by κ_{chem} (with the ratio of κ_{chem} to κ_{gf} of ~0.8). Similar patterns were also noted by Zhang et al., (2017) but which is only based on a comparison between κ_{chem} derived from bulk chemical composition and κ_{gf} . Our results based on size-resolved measurements are consistent with that observed by Zhang et al., (2017), and thus again indicate that confirming an effect of the rapid photochemical aging of BC aerosol particles, ~~which are generally with dominant size modes of 100-200 nm in the atmosphere, may lead to the core shell structure in which certain secondary aerosol generated from photochemical reactions is thickly coated on the surface of BC (Wang et al., 2019). The on their~~ hygroscopicity ~~of the coated BC particles may only depend on the coating layer (Ma et al., 2013), thus resulting in the noontime/early afternoon underestimation of particle hygroscopicity by κ_{chem} .~~ While, no significant differences between κ_{chem} and κ_{gf} are observed during night time in summer. Note that κ_{chem} is slightly higher than κ_{gf} during early evening traffic rush hour and cooking time, when emissions of primary hydrophobic particles (e.g. BC and POA) are high (Fig. 3), thus resulting in a large percentage of externally-mixed particles). Causes of the overestimation in κ_{chem} during the traffic rush hour and cooking time will be discussed in the following paragraph. The particles experience rapid conversion and mixing in urban Beijing due to high precursor gases (Sun et al., 2015; Wu et al., 2016; Ren et al., 2018), ~~and thus the coated/aged particles produced through photochemical processing processes~~ in the afternoon can mix and interact with ~~and the~~ freshly emitted primary particles ~~emitted during rush hour from traffic and cooking sources~~ (Wu et al., 2008). Therefore, during nighttime (22:00-06:00, LT), the particles are more uniform and internally-mixed, which is reflective of the assumption for calculation of κ_{chem} , a much better consistency between κ_{chem} and κ_{gf} is observed, hence presented.

带格式的: 字体颜色: 文字 1, 英语(美国)

带格式的: 字体颜色: 文字 1

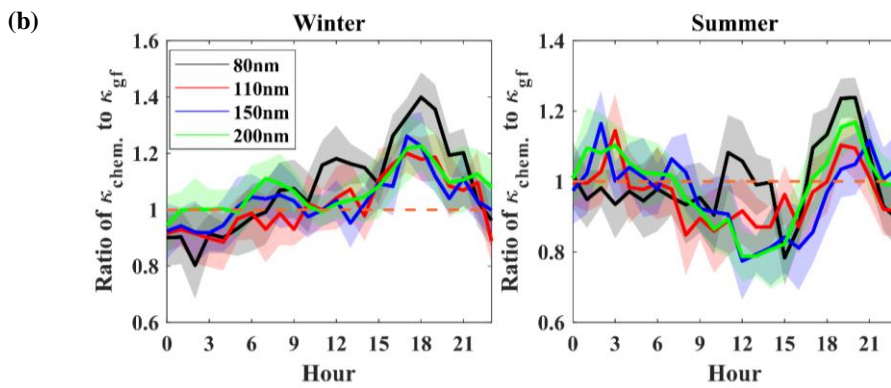
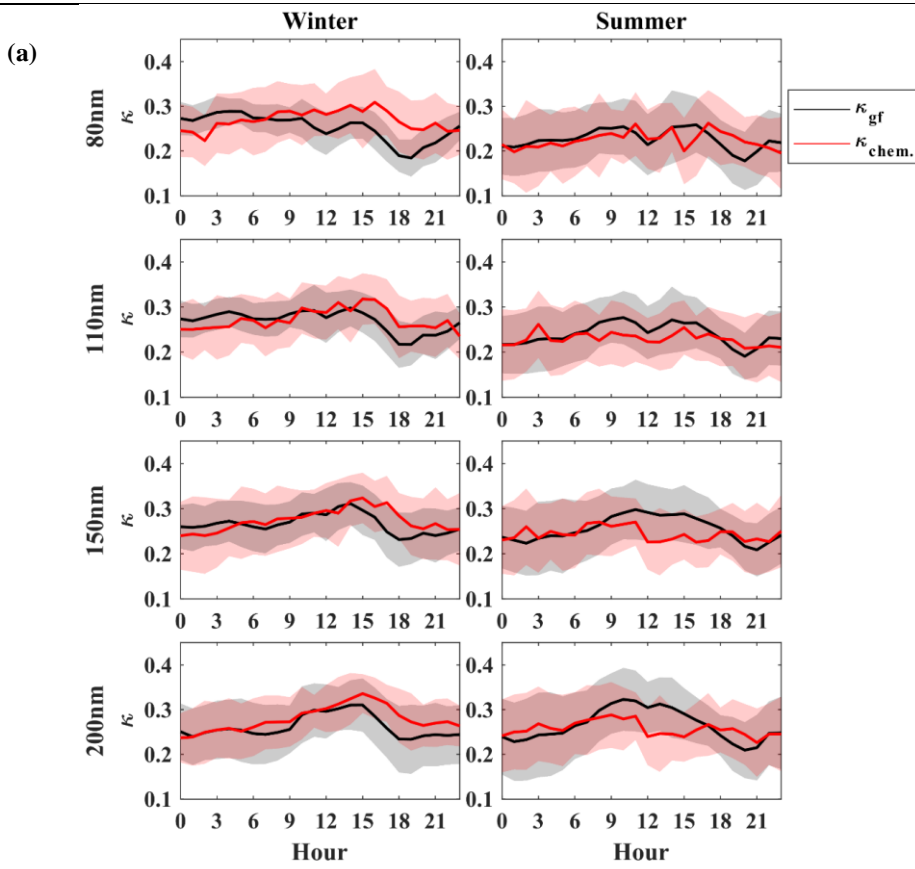


Figure 6. Diurnal variations of (a) κ_{chem} using size-resolved chemical composition data and κ_{gf} in winter and summer period; and (b) ratio of κ_{chem} to κ_{gf} in winter and summer period. The shade regions denote the error bars (1σ).

In winter, the disparity between κ_{chem} to κ_{gf} is insignificant at 09:00-15:00 due to the weakening effect of photochemical aging. From 15:00 to 21:00 LT, due to the strong vehicle and cooking sources around the site, the particles are dominated by the hydrophobic mode with a large concentration of externally-mixed BC and POA particles (Fig. 3), the calculated κ_{chem} is much higher than κ_{gf} , with the maximum ratio of κ_{chem} to κ_{gf} of 1.2-1.4, and the greatest disparity is observed for small particles. The disparity is further enhanced during clean periods when the hydrophobic mode is dominant (Fig. 7, Fig. S1). Note that during the nighttime, κ_{chem} is slight lower than κ_{gf} , with the minimum ratio of κ_{chem} to κ_{gf} of ~ 0.8 for 80 nm particles and ~ 0.9 for 110 and 150 nm particles at 02:00-04:00 LT (Fig. 6b), indicating an underestimation of particle hygroscopicity using composition data. The disparity at nighttime is further increased during heavily polluted events (Fig. S1), when the particles are more internally-mixed with only one hygroscopic mode (Fig. 7). We propose the increased underestimation during polluted conditions is likely due to enhanced condensation of secondary hygroscopic compounds (e.g. nitrate, sulfate, SOA) on pre-existing aerosols at lower temperature and/or hydrophilic SOA formation under higher relative humidity at nighttime (Wu et al., 2008; Wang et al., 2016; An et al., 2019). However, such condensation effect during nighttime is less significant (indicated by the smaller disparity between κ_{chem} and κ_{gf}) than the aging effect caused by aerosols photochemical processes around noontime (Peng et al., 2016b).

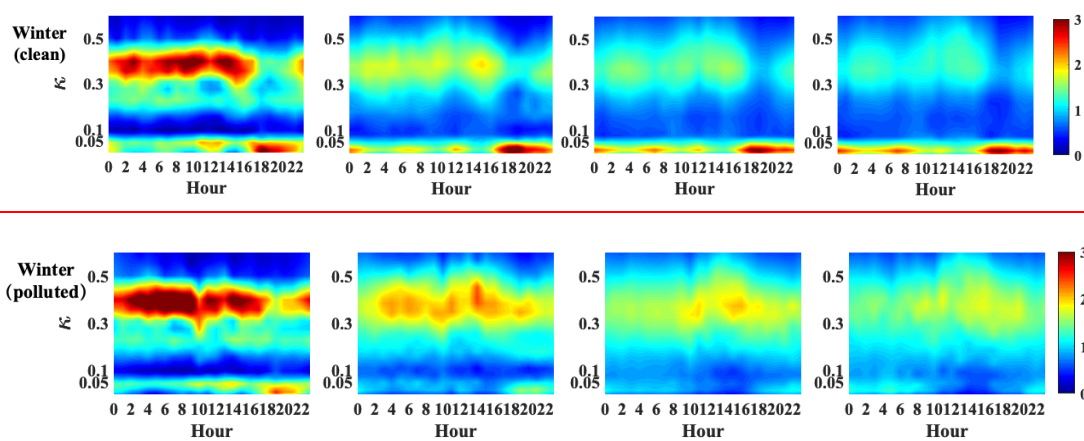


Figure 7. Diurnal cycles of κ_{gf} -PDF for 80, 110, 150 and 200 nm particles in clean and polluted events in winter.

We suppose that the ~~large disparity between~~ higher/lower κ_{chem} and κ_{gf} ~~is due to~~ should be firstly closely associated with temporal ~~variations~~ changes in actual effective density of BC ~~and organics caused by~~ with the particles aging ~~and~~ diurnal variations of local ~~sources~~ emissions. It has been demonstrated that rapid aging of BC can occur over a few hours in the polluted urban area (Peng et al., 2016b). The externally-mixed BC particles are with fractal structure and chain-like aggregates and have been reported with effective density of 0.25-0.45 g cm⁻³ (McMurry et al., 2002), ~~While~~ while the BC particles in the κ_{chem} calculation is assumed as void free with effective density of 1.7 g cm⁻³. ~~Such inappropriate assumption would lead~~ This leads to ~~an underestimation of~~ less BC volume fraction than it actually is and thus the ~~overestimation in~~ greater κ_{chem} during the traffic rush hour and cooking time when BC particles are mostly freshly emitted with uncompact structure. In addition, the significant increase in volume fraction of POA during the late afternoon would result in changes of composition of organic aerosols and thereby a ~~lower~~ density of ~~organics, which is expected~~ much closer to ~~be smaller~~ that of POA than the assumed one (1.2 g cm⁻³) in the calculation should be applied. A sensitivity test has been done to examine the effect of density of BC and organics on calculated κ_{chem} (Fig. 78). The result shows that the κ_{chem} value ~~reduces~~ can be reduced by 16-33% ~~when applying~~ by decreasing the BC effective density ~~offrom~~ from 1.7 g cm⁻³ to 0.25-0.45 g cm⁻³. This basically explains the disparity between κ_{chem} and κ_{gf} during the traffic rush hour. ~~However, the~~ when a large amount of BC is freshly emitted. The changes in κ_{chem} are within $\pm 4\%$ ~~when changing~~ by varying the organic density from 1.0 (typical 2 (mixture of SOA and POA) to 1.0 (typically for POA) ~~to~~ or 1.4 (typical g cm⁻³ (typically for SOA) g cm⁻³, ~~suggesting insensitivity of κ_{chem} to~~ (Zamora et al., 2019), showing much ~~less impacts of~~ variations of organic density. ~~The~~ on κ_{chem} . In conclusion, ~~the~~ result also demonstrated that the disparity between κ_{chem} and κ_{gf} during late afternoon in winter is largely due to the inappropriate use of the BC particles density that is closely associated with its morphology or degree of its aging. Our study suggest that, to accurately parameterize the effect of BC aging on particles hygroscopicity, it is critical to measure the effective density and morphology of ambient BC, in particularly in those regions with complex influences of rapid secondary conversion/aging processes and local sources.

In that way, the lower κ_{chem} value derived around noontime in summer, when BC aerosols may be more compact through strong photochemical aging, is probably due to application of a lower BC density in the calculation. However, the sensitivity test indicates that, to fill the gap between κ_{chem} and κ_{gf} observed at noontime in summer, the effective density of BC should be extremely high due to the decreased sensitivity of κ_{chem} to BC density with their aging of BC. In this case, the density of BC has been assumed density of BC is as 1.7 g cm⁻³, which reflects a very compacted and void free structure of the BC particles. The current/This currently applied value represents an upper limit for the effective density of ambient BC particles according to previous observations at a site near urban or in Beijing (Zhang et al., 2015), which suggested the aged BC is generally with effective density of 1.2-1.4 g cm⁻³. Using these ambient observed density values would lead to further underestimation in κ_{chem} . Our results exhibit the increase. In addition, the photochemical aging can change the overall effective density of the organic aerosols through changing their chemical composition. However, the effective density of the photochemical oxidized organic particles (e.g. SOA) does not change much on the timescale of several hours, and was observed ranging between 1.2 and 1.3 g cm⁻³ (Bahreini et al., 2005). It can only explain ~4% at most of the underestimation in κ_{chem} around noontime in summer by applying a density value of 1.4 g cm⁻³ (typically for SOA). Therefore, application of higher densities of BC and organics in the calculation cannot fully explain the disparity between κ_{chem} and κ_{gf} observed around noontime during early afternoon in summer. This just, on the other hand, verifies the when strong photochemical processes are expected.

The uncertainty in calculation of κ_{chem} may be also related to the uncertainty caused by hygroscopic parameter of organics that vary widely over a range of diverse constituents of SOA (Suda et al., 2012). aging/coating effect. The lower κ_{chem} indicates that the κ of secondary organic aerosols formed through the strong photochemical oxidation processes in summer of urban Beijing are likely underestimated. In this study, the mean κ value of organics derived from the f_{44} parametrized equation is 0.20 ± 0.02 , ranging from 0.17 to 0.23 during 09:00-17:00. While the organic aerosols, especially for particles in accumulated mode, may be more hydrophilic with much larger κ , i.e. >0.2 due to large formation of highly-oxidized OA. One can easily get that increasing the κ of organic aerosols from 0.2 to 0.3 can explain about 11-13%

带格式的: 字体颜色: 自动设置

带格式的: 字体颜色: 自动设置

带格式的: 字体颜色: 文字 1

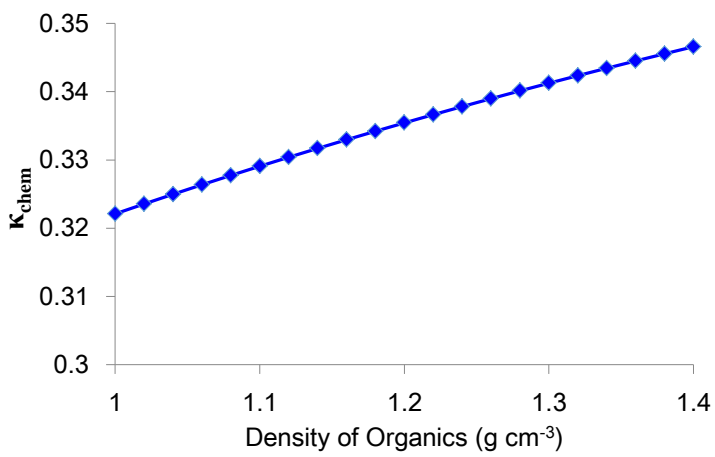
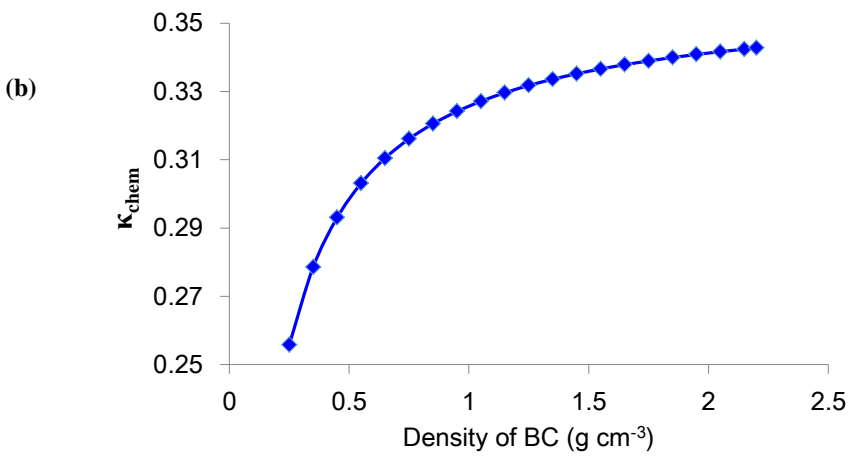
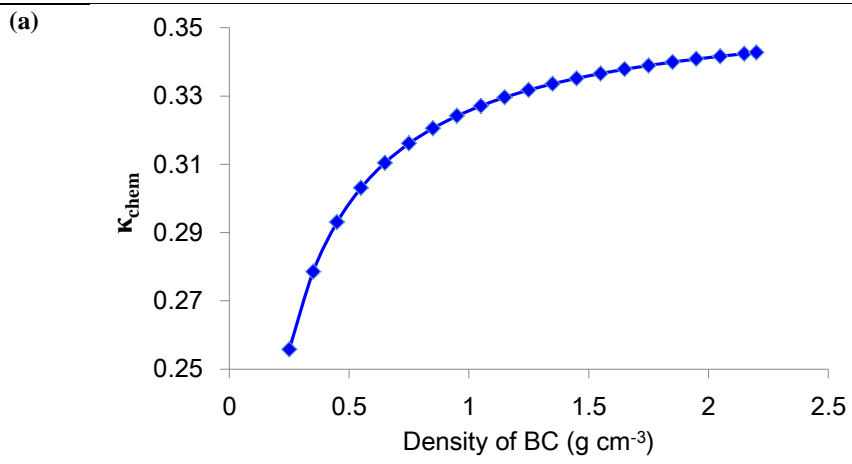
带格式的: 字体颜色: 文字 1

带格式的: 字体颜色: 文字 1

400 underestimation of κ_{chem} , but representing an upper limit of the impact of hygroscopicity of organic aerosols,
401 on the aerosols hygroscopicity. In addition calculation. This is because that the κ value of 0.3 corresponds to
402 the maximum possible for ambient organic aerosols. Additionally, the f_{44} parametrized equation tends to
403 overestimate the κ according to Fröhlich et al. (2015), which should yield a larger κ_{chem} . Finally, the
404 coexisting hygroscopic and hydrophobic species may have a strong influence on the phase state of particles,
405 also likely affecting chemical interactions between inorganic and organic compounds as well as the overall
406 hygroscopicity of mixed particles (Peng et al., 2016). Further investigations are needed to verify this. Our
407 study suggest that, to accurately parameterize the effect of BC aging on particles hygroscopicity, future
408 investigations need to measure the effective density and morphology of ambient BC, in particularity in those
409 regions with complex local sources (2016a). Overall, The lower κ_{chem} caused by the photochemical aging
410 effect is likely resulted from multiple impacts of inappropriate application of density and hygroscopic
411 parameter of organic aerosols in the calculation, as well as the influences from chemical interaction between
412 organic and inorganic compounds on the overall hygroscopicity of mixed particles. This topic warrants
413 further investigations.

带格式的: 字体颜色: 文字 1

带格式的: 字体颜色: 自动设置.



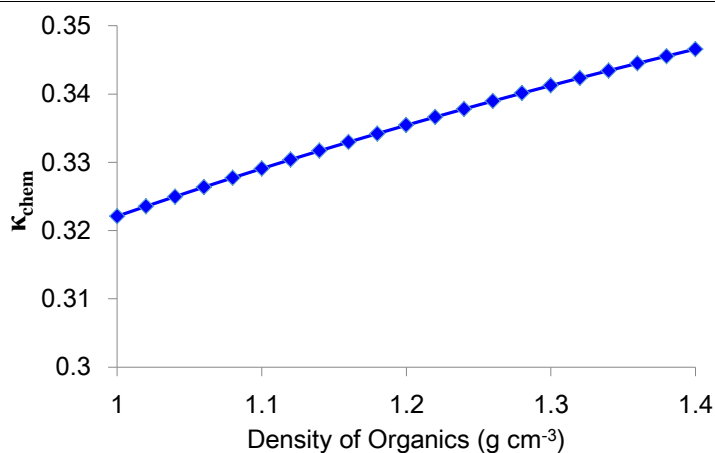


Figure 8. Sensitivity of κ_{chem} to variations of density of BC (a) and organics (b)

Besides the impacts of BC aging (changes in morphology/density) and variations of the overall density of organics on particles hygroscopicity, uncertainty in κ_{chem} may be related to the uncertainty in the hygroscopic parameter for organics that could vary widely over a range of diverse constituents of SOA (Suda et al., 2012). However, Zhang et al. (2017) shown that using a smaller or larger κ_{SOA} could not fully explain the overestimation during traffic hours or the underestimation around noontime. Furthermore, in this study, it is calculated from a simple parametrized equation based on the AMS measured f_{44} value reported by Mei et al. (2013). The value for f_{44} tends to be overestimated according to Fröhlich et al. (2015), which should yield a larger κ_{chem} . Previous studies have shown that freshly emitted POA and BC particles may be rapidly coated by more hygroscopic components in polluted urban areas, resulting in enhanced hygroscopicity of the mixed particles (Zhang et al., 2004; Johnson et al., 2005; Zhao et al., 2017). Our results are consistent with those observations and clarify the photochemical aging and coating effect will largely underestimate the particles hygroscopicity using simple mixing rule based on chemical composition.

Note that during the nighttime, κ_{chem} is slight lower than κ_{gf} , with the minimum ratio of κ_{chem} to κ_{gf} of 0.8 for 80 nm particles and 0.9 for 110 and 150 nm particles at 02:00–04:00 LT (Fig. 6b), indicating an underestimation of particle hygroscopicity using composition data. The disparity at nighttime is further

increased during heavily polluted events (Fig. S1), when the particles are more internally mixed with only one hygroscopic mode (Fig. 8). We propose the increased underestimation during polluted conditions is likely due to enhanced condensation of secondary hygroscopic compounds (e.g. nitrate, sulfate) on pre-existing aerosols at lower temperature and higher relative humidity at nighttime (Wu et al., 2008; Wang et al., 2016; An et al., 2019). However, such condensation effect during nighttime is less significant (indicated by the smaller disparity between κ_{chem} and κ_{gf}) than the coating effect caused by aerosols photochemical aging at noontime, likely due to thinner coating layer formed on the pre-exist particles during nighttime or other factors influencing the particles hygroscopicity.

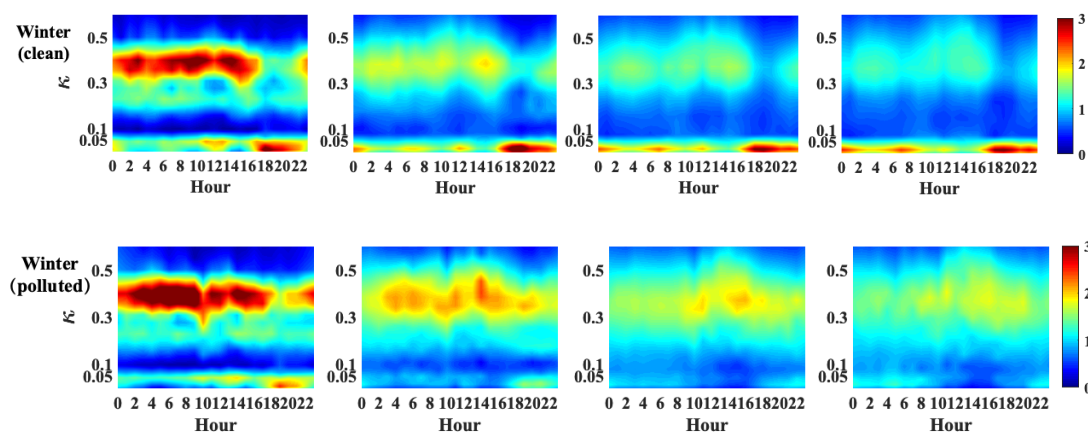


Figure 8. Diurnal cycles of κ_{gf} - PDF for 80, 110, 150 and 200 nm particles in clean and polluted events in winter.

3.5. Observation from other stations

The aging process in the summer period is related to photochemical processing in strong solar radiation conditions. The photochemical reactions produce sulfate and secondary organic aerosol, condensing on the surface of slightly- or non-hygroscopic primary aerosols (such as BC) (Zhang et al., 2008). As discussed in 3.4, the core-shell structure that accompanies aging of the particles results in calculated κ_{chem} that underestimates their hygroscopicity. To confirm such a coating effect on particle hygroscopicity, we further examine the diurnal variations of κ_{chem} and κ_{gf} or κ_{CCNc} (only at XZ site)

454 based on observations in summer at two other sites in north China (Fig. 1). The XT site is located in the
455 suburb of XT city, which is about 400 km south of Beijing, with high levels of industrialization and
456 urbanization. Due to industrial emissions and typically weak ventilating winds, concentrations of PM_{2.5},
457 black carbon and gaseous precursors are usually high at the site (Fu et al., 2014). Xinzhou is located in north
458 of Taiyuan and about 360 km southwest of Beijing, and is surrounded by mountains on three sides. Local
459 emissions from motor vehicles and industrial activities have relatively little influence on the sampled aerosol
460 (Zhang et al., 2016). Because of its location and elevation, the aerosol at the XZ site is usually aged and
461 transported from other areas. The sampling period was from July 22 to August 26, 2014 and from May 17 to
462 June 14, 2016 at XZ and XT site respectively.

463 We find that the case at the XT site is very similar to that observed in BJ (Fig. 9a), with a lower κ_{chem}
464 than κ_{gf} around noon time. But, because of much less influences from the local sources at XT compared to
465 that at BJ, such underestimation by κ_{chem} continued until night at XT (Fig. 9b). Interestingly, a noontime
466 lower κ_{chem} was not observed in the diurnal cycles at the XZ site, where κ_{chem} and κ_{CCNc} had similar diurnal
467 patterns (Fig. 9c) with a roughly constant ratio of κ_{chem} to κ_{CCNc} of ~0.8-0.9 (Fig. 9d). This is probably
468 because the XZ site is usually the recipient of aerosols transported from other areas that are already aged and
469 well-mixed, with minimal impact of ~~additional coating~~ further aging (Zhang et al., 2017). Also, the rate of
470 oxidation and condensation may be slow in the relatively remote area where the gas precursors and oxidants
471 are not as high as they are closer to sources regions. But at XT, which is located in the heavily polluted area
472 in the north China Plain (Fu et al., 2014), aerosol emissions and processing are more similar to that in urban
473 Beijing. These observations from other sites further confirms the the photochemical aging ~~and coating~~
474 that will largely underestimate the particles hygroscopicity using simple mixing rule based on chemical
475 composition. _

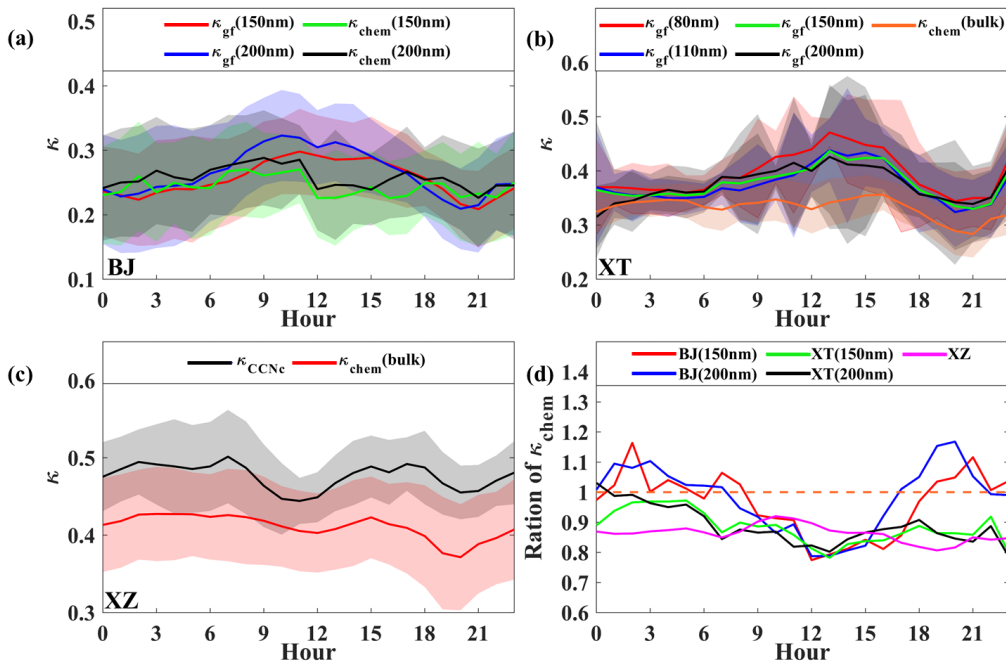


Figure 9. Diurnal variations in (a) κ_{chem} and κ_{gf} for 150 and 200 nm particles at BJ site; (b) κ_{chem} and κ_{gf} for 40, 80, 110, 150 and 200 nm particles at XT site; (c) κ_{chem} and mean κ_{CCNe} for particles at XZ site, and (d) ratio of mean κ_{chem} to κ_{gf} at the three sites.

4. Conclusion

Using measurements of aerosol composition and hygroscopicity made in Beijing (BJ) during a winter period of 2016 and a summer period of 2017, this paper analyzes the daily variation and seasonal differences of size-resolved aerosol hygroscopicity in urban Beijing. We mainly focus on studying the disparity of κ_{gf} and κ_{chem} between summer and winter to reveal the impact of atmospheric processes and mixing state of the particles on its hygroscopicity. The uncertainty in calculating κ by using chemical composition with a uniform internal mixing hypothesis is elucidated from the diurnal variations of the difference between the calculated values: in summer, lower κ_{chem} is obtained around noontime, with a ratio of κ_{chem} to κ_{gf} of about 0.8-0.9 for large particles (i.e. 150 nm and 200 nm), showing an underestimation of particles hygroscopicity by using simple mixing rule based on chemical composition. Combining with the observation from XT and

490 XZ, we attribute the underestimation to the rapid noontime photochemical aging processes in summer,
491 which induces the ~~coatingaging~~ effect that will lead to a lower κ if assuming a uniform mixing of the
492 particles. ~~The lower κ_{chem} is likely resulted from multiple impacts of inappropriate application of density and~~
493 ~~hygroscopic parameter of organic aerosols in the calculation, as well as the unknown influences from~~
494 ~~chemical interaction between organic and inorganic compounds on the overall hygroscopicity of mixed~~
495 ~~particles.~~

496 In ~~contrast~~winter, larger κ_{chem} than κ_{gf} for >100 nm particles ~~is derived~~ around noontime and in the early
497 afternoon ~~is derived in winter~~, with the maximum ratio of κ_{chem} to κ_{gf} of 1.2-1.4 when the particles are
498 dominated by the hydrophobic mode with a large number of externally-mixed POA particles from strong
499 vehicle and cooking sources. We attribute this large disparity between κ_{chem} and κ_{gf} to changes of BC
500 morphology that can be indicated by effective density of BC. The sensitivity test shows that it can well
501 explain the disparity during the traffic rush hour by applying BC effective density of 0.25-0.45 g cm⁻³.

502 However, we suggest that,

503 to accurately parameterize or account for the effect of BC density on particles hygroscopicity, future
504 investigations need to measure the effective density of ambient BC, in particularity in those regions with
505 complex local sources.

506 ~~A lower κ_{chem} than κ_{gf} for 80, 110 and 150 nm particles during the nighttime of winter is also noted, and~~
507 ~~the disparity is further enlarged in polluted days, probably due to a nighttime coating effect driven by~~
508 ~~condensation of secondary hygroscopic species on pre-existing aerosols in cold season.~~ Our results highlight
509 the impacts of atmospheric processes, sources on aerosol mixing state and hygroscopicity, which should be
510 quantified and considered in models for different atmospheric conditions.

511
512 *Data availability.* All data needed to evaluate the conclusions in the paper are present in the paper and/or the
513 Supplementary Materials. Also, all data used in the study are available from the corresponding author upon
514 request (fang.zhang@bnu.edu.cn).

515 *Author contributions.* F.Z. and J. L conceived the conceptual development of the manuscript. X. F. directed
516 and performed of the experiments with L.C., X.J., Y. W., and F. Z.. F.Z., J.L., and X.F. conducted the data
517 analysis and wrote the draft of the manuscript, and all authors edited and commented on the various sections
518 of the manuscript. J.L. and X.F. contribute equally to this work.

519 *Competing interests.* The authors declare no competing interests.

520 *Acknowledgements.* This work was funded by National Natural Science Foundation of China (NSFC)
521 research projects (grant nos. 41975174, 41675141, 91544217), the National Key R&D Program of China
522 (grant no. 2017YFC1501702). We thank all participants of the field campaign for their tireless work and
523 cooperation. [We also would like to thank the two anonymous reviewers for their insightful and constructive](#)
524 [comments.](#)

525 **References**

526 An, Z., Huang, R. J., Zhang, R., Tie, X., Li, G., Cao, J., Zhou, W., Shi, Z., Han, Y., Gu, Z., and Ji, Y.:
527 Severe haze in Northern China: A synergy of anthropogenic emissions and atmospheric processes,
528 Proceedings of the National Academy of Sciences, 116(18), 8657-8666, doi:10.1073/pnas.1900125116,
529 2019.

530 [Bahreini, R., Keywood, M. D., Ng, N. L., Varutbangkul, V., and Jimenez, J. L.: Measurements of secondary](#)
531 [organic aerosol from oxidation of cycloalkenes, terpenes, and *m*-xylene using an aerodyne aerosol mass](#)
532 [spectrometer. *Environ. Sci. Technol.*, 39\(15\), 5674–5688, 2005.](#)

533 Bougiatioti, A., Fountoukis, C., Kalivitis, N., Pandis, S. N., Nenes, A., and Mihalopoulos, N.: Cloud
534 condensation nuclei measurements in the marine boundary layer of the Eastern Mediterranean: CCN
535 closure and droplet growth kinetics, *Atmos. Chem. Phys.*, 9, 7053–7066, doi: 10.5194/acp-9-7053-2009,
536 2009.

537 Carrico, C. M., M. D. Petters, S. M. Kreidenweis, J. L. Collett Jr., G. Engling, and Malm W. C.: Aerosol
538 hygroscopicity and cloud droplet activation of extracts of filters from biomass burning experiments, *J.*
539 *Geophys. Res.*, 113, D08206, doi:10.1029/2007JD009274. 2008.

540 Cerully, K. M., Raatikainen, T., Lance, S., Tkacik, D., Tiitta, P., Petäjä T., Nenes, A. : Aerosol
541 hygroscopicity and CCN activation kinetics in a boreal forest environment during the 2007 EUCAARI
542 campaign, *Atmos. Chem. Phys.*, 11, 12369–12386, doi: 10.5194/acp-11-12369-2011, 2011.

543 Chang, R.-W., Liu, P., Leaitch, W., and Abbatt, J.: Comparison between measured and predicted CCN
544 concentrations at Egbert, Ontario: Focus on the organic aerosol fraction at a semi-rural site, *Atmos.*
545 *Environ.*, 41, 8172–8182, 2007.

546 Collins, D. R., Flagan, R. C., and Seinfeld, J. H.: Improved inversion of scanning DMA data, *Aerosol Sci.*
547 *Technol.*, 36(1), 1–9, 2002.

548 Cruz, C. N. and Pandis, S. N.: Deliquescence and hygroscopic growth of mixed inorganic-organic
549 atmospheric aerosol, *Environ. Sci. Technol.*, 34, 4313–4319, doi: 10.1021/es9907109, 2000.

550 DeCarlo, P. F., Kimmel, J. R., Trimborn, A., Northway, M. J., Jayne, J. T., Aiken, A. C., Gonin, M., Fuhrer,
551 K., Horvath, T., Docherty, K., Worsnop, D. R., and Jimenez, J. L.: Field-deployable, high-resolution,
552 time-of-flight aerosol mass spectrometer, *Anal. Chem.*, 78, 8281–8289, doi: 10.1021/ac061249n, 2006.

553 Fors, E. O., Swietlicki, E., Svenningsson, B., Kristensson, A., Frank, G. P., and Sporre, M.: Hygroscopic
554 properties of the ambient aerosol in southern Sweden – a two year study, *Atmos. Chem. Phys.*, 11, 8343–
555 8361, doi: 10.5194/acp-11-8343-2011, 2011.

556 Fröhlich, R., Crenn, V., Setyan, A., Belis, C. A., Canonaco, F., Favez, O., Riffault, V., Slowik, J. G.,
557 Aas, W., Aijälä M., Alastuey, A., Artañano, B., Bonnaire, N., Bozzetti, C., Bressi, M., Carbone, C., Coz,
558 E., Croteau, P. L., Cubison, M. J., Esser-Giel, J. K., Green, D. C., Gros, V., Heikkinen, L., Herrmann, H.,
559 Jayne, J. T., Lunder, C. R., Minguillón, M. C., Mocnik, G., O’Dowd, C. D., Ovadnevaite, J., Petralia, E.,
560 Poulain, L., Priestman, M., Ripoll, A., Sarda-Estève, R., Wiedensohler, A., Baltensperger, U., Sciare, J.,
561 and Prévôt, A. S. H.: ACTRIS ACSM intercomparison – Part 2: Intercomparison of ME-2 organic source
562 apportionment results from 15 individual, co-located aerosol mass spectrometers, *Atmos. Meas. Tech.*, 8,
563 2555–2576, doi:10.5194/amt-8-2555-2015, 2015.

564 Fu, G. Q., Xu, W. Y., Yang, R. F., Li, J. B., & Zhao, C. S. : The distribution and trends of fog and haze in
565 the North China Plain over the past 30 years, *Atmos. Chem. Phys.*, 14, 11949-11958, doi:
566 10.5194/acp-14-11949-2014, 2014.

567 Gasparini, R., R. Li, and D. R. Collins: Integration of size distributions and size-resolved hygroscopicity
568 measured during the Houston Supersite for compositional categorization of the aerosol, *Atmos. Environ.*,
569 38, 3285–3303, doi:10.1016/j.atmosenv.2004.03.019, 2004.

570 Good, N., Topping, D. O., Allan, J. D., Flynn, M., Fuentes, E., Irwin, M., Williams, P. I., Coe, H., and
571 McFiggans, G.: Consistency between parameterisations of aerosol hygroscopicity and CCN activity
572 during the RHaMBLe discovery cruise, *Atmos. Chem. Phys.*, 10, 3189–3203, doi:
573 10.5194/acp-10-3189-2010, 2010.

574 Gunthe, S. S., King, S. M., Rose, D., Chen, Q., Roldin, P., Farmer, D. K., Jimenez, J. L., Artaxo, P., Andreae,
575 M. O., Martin, S.T., and Pöschl, U.: Cloud condensation nuclei in pristine tropical rainforest air of
576 Amazonia: size-resolved measurements and modeling of atmospheric aerosol composition and CCN
577 activity, *Atmos. Chem. Phys.*, 9, 7551–7575, doi: 10.5194/acp-9-7551-2009, 2009.

578 Gysel, M., Crosier, J., Topping, D. O., Whitehead, J. D., Bower, K.N., Cubison, M. J., Williams, P. I., Flynn,
579 M. J., McFiggans, G.B., and Coe, H.: Closure study between chemical composition and hygroscopic
580 growth of aerosol particles during TORCH2, *Atmos. Chem. Phys.*, 7, 6131–6144, doi:
581 10.5194/acp-7-6131-2007, 2007.

582 Gysel, M., McFiggans, G. B., and Coe, H.: Inversion of tandem differential mobility analyser (TDMA)
583 measurements, *J. Aerosol Sci.*, 40, 134–151, doi: 10.1016/j.jaerosci.2008.07.013, 2009.

584 Hu, W., Hu, M., Hu, W., Jimenez, J. L., Yuan, B., Chen, W., Wang, M., Wu, Y., Chen, C., Wang, Z., Peng,
585 J., Zeng, L., and Shao, M.: Chemical composition, sources, and aging process of submicron aerosols in
586 Beijing: Contrast between summer and winter, *J. Geophys. Res.*, 121, 1955–1977, doi:
587 10.1002/2015JD024020, 2016.

588 Irwin, M., Good, N., Crosier, J., Choularton, T. W., & McFiggans, G.: Reconciliation of measurements of
589 hygroscopic growth and critical supersaturation of aerosol particles in central Germany Atmos. Chem.
590 Phys., 10, 11737–11752, doi:10.5194/acp-10-11737-2010, 2010.

591 Jacobson, M.Z. : Strong radiative heating due to the mixing state of black carbon in atmospheric aerosols,
592 Nature, 409(6821):695-697, 2001.

593 ~~Johnson, K. S., Zuberi, B., Molina, L. T., Molina, M. J., Iedema, M. J., Cowin, J. P., Gaspar, D. J., Wang, C.,
594 and Laskin, A.: Processing of soot in an urban environment: Case study from the Mexico City
595 Metropolitan Area, Atmos. Chem. Phys., 5, 3033–3043, doi: 10.5194/acp-5-3033-2005, 2005.~~

596 Kulmala, M., Petaja, T., Monkkonen, P., Koponen, I.K., Dal Maso, M., Aalto, P.P., Lehtinen, K.E.J., and
597 Kerminen, V.M. : On the growth of nucleation mode particles: source rates of condensable vapor in
598 polluted and clean environments, Atmos. Chem. Phys., 5, 409–416, doi: 10.5194/acp-5-409-2005, 2005.

599 Kuwata, M., Kondo, Y., Miyazaki, Y., Komazaki, Y., Kim, J. H., Yum, S. S., Tanimoto, H., and Matsuedda,
600 H.: Cloud condensation nuclei activity at Jeju Island, Korea in spring 2005, Atmos. Chem. Phys., 8,
601 2933–2948, doi:10.5194/acp-8-2933-2008, 2008.

602 Liu, D., Joshi, R., Wang, J., Yu, C., Allan, J. D., Coe, H., Flynn, M. J., Xie, C., Lee, J., Squires, F., Kotthaus,
603 S., Grimmond, S., Ge, X., Sun, Y., and Fu, P.: Contrasting physical properties of black carbon in urban
604 Beijing between winter and summer, Atmos. Chem. Phys. Discuss., doi: 10.5194/acp-2018-1142, in
605 review, 2018.

606 Liu, P. F., Zhao, C. S., Göbel, T., Hallbauer, E., Nowak, A., Ran, L., Xu, W. Y., Deng, Z. Z., Ma, N.,
607 Mildnerberger, K., Henning, S., Stratmann, F., and Wiedensohler, A.: Hygroscopic properties of aerosol
608 particles at high relative humidity and their diurnal variations in the North China Plain, Atmos. Chem.
609 Phys., 3479–3494, doi:10.5194/acp-11-3479-2011, 2011.

610 Ma, Y., Brooks, S. D., Vidaurre, G., Khalizov, A. F., Wang, L., and Zhang, R.: Rapid modification of
611 cloud-nucleating ability of aerosols by biogenic emissions, Geophys. Res. Lett., 40, 6293–6297, doi:
612 10.1002/2013GL057895, 2013.

带格式的: 字体颜色: 黑色, 图案: 清除 (白色)

带格式的: 字体颜色: 黑色, 图案: 清除 (白色)

带格式的: 字体颜色: 黑色, 图案: 清除 (白色)

- 613 Massling, A., Stock, M., and Wiedensohler, A.: Diurnal, weekly, and seasonal variation of hygroscopic
614 properties of submicrometer urban aerosol particles, *Atmos. Environ.*, 39(21), 3911–3922, doi:
615 10.1016/j.atmosenv.2005.03.020, 2005.
- 616 McMurry, P. H.; Wang, X.; Park, K.; Ehara, K. The Relationship between Mass and Mobility for
617 Atmospheric Particles. *Aerosol Sci. Technol.*, 36, 227-238, 2002.
- 618 Mei, F., Hayes, P. L., Ortega, A. M., Taylor, J. W., Allan, J. D., Gilman, J. B., Kuster, W. C., de Gouw, J. A.,
619 Jimenez, J. L., and Wang, J.: Droplet activation properties of organic aerosols observed at an urban site
620 during CalNex-LA, *J. Geophys. Res.*, 118, 2903–2917, doi: 10.1002/jgrd.50285, 2013.
- 621 Mikhailov, E. F., Mironov, G. N., Pöhlker, C., Chi, X., Krüger, M. L., Shiraiwa, M., Förster, J. D., Pöschl,
622 U., Vlasenko, S. S., Ryshkevich, T. I., Weigand, M., Kilcoyne, A. L. D., and Andreae, M. O.: Chemical
623 composition, microstructure, and hygroscopic properties of aerosol particles at the Zotino Tall Tower
624 Observatory (ZOTTO), Siberia, during a summer campaign, *At-mos. Chem. Phys.*, 15, 8847–8869,
625 doi:10.5194/acp-15-8847-2015, 2015.
- 626 Peng, C., Jing, B., Guo, Y. C., Zhang, Y. H., and Ge, M. F.: Hygroscopic behavior of multicomponent
627 aerosols involving nacl and dicarboxylic acids. *J. Phys. Chem. A*, 120(7), 1029-1038, [20162016a](#).
- 628 Peng, J. F., Hu, M., Guo, S., Du, Z., Shang, D., and Zheng, J.: Ageing and hygroscopicity variation of
629 black carbon particles in beijing measured by a quasi-atmospheric aerosol evolution study (quality)
630 chamber. *Atmospheric Chemistry and Physics*, 17(17), 10333-10348, [20172017a](#).
- 631 [Peng, J. F., Hu, M., Du, Z. F., Wang, Y. H., Zheng, J., Zhang, W. B., Yang, Y. D., Qin, Y. H., Zheng, R.,](#)
632 [Xiao, Y., Wu, Y. S., Lu, S. H., Wu, Z. J., Guo, S., Mao, H. J., and Shuai, S. J.: Gasoline aromatics: a](#)
633 [critical determinant of urban secondary organic aerosol formation. *Atmospheric Chemistry and Physics*,](#)
634 [17, 10743-10752, 2017b.](#)
- 635 [Peng, J. F., Hu, M., Wang, Z. B., Huang, X. F., Kumar, P., Wu, Z. J., Guo, S., Yue, D. L., Shang, D. J.,](#)
636 [Zheng, Z., and He, L. Y.: Submicron aerosols at thirteen diversified sites in China: size distribution, new](#)
637 [particle formation and corresponding contribution to cloud condensation nuclei production, *Atmospheric*](#)
638 [Chemistry and Physics, 14, 10249-10265, DOI 10.5194/acp-14-10249-2014, 2014.](#)

带格式的: 字体颜色: 黑色, 图案: 清除 (白色)

带格式的: 字体颜色: 黑色, 图案: 清除 (白色)

带格式的: 字体颜色: 黑色, 图案: 清除 (白色)

带格式的: 字体颜色: 黑色, 图案: 清除 (白色)

639 [Peng, J. F., Hu, M., Guo, S., Du, Z. F., Zheng, J., Shang, D. J., Zamora, M. L., Zeng, L. M., Shao, M., Wu,](#)
640 [Y. S., Zheng, J., Wang, Y., Glen, C. R., Collins, D. R., Molina, M. J., and Zhang, R. Y.: Markedly](#)
641 [enhanced absorption and direct radiative forcing of black carbon under polluted urban environments, P](#)
642 [Natl Acad Sci USA, 113, 4266-4271, 10.1073/pnas.1602310113, 2016b.](#)

643 Petters, M. D. and Kreidenweis, S. M.: A single parameter representation of hygroscopic growth and cloud
644 condensation nucleus activity, *Atmos. Chem. Phys.*, 7, 1961–1971, doi: 10.5194/acp-7-1961-2007, 2007.

645 Ren, J. Y., Zhang, F., Wang, Y. Y., Collins, D., Fan, X. X., Jin, X. A., Xu, W. Q., Sun, Y. L., Cribb, M., and
646 Li, Z. Q.: Using different assumptions of aerosol mixing state and chemical composition to predict CCN
647 concentrations based on field measurements in urban Beijing, *Atmos. Chem. Phys.*, 18, 6907–6921, doi:
648 10.5194/acp-18-6907-2018, 2018.

649 Rose, D., Nowak, A., Achtert, P., Wiedensohler, A., Hu, M., Shao, M., Zhang, Y., Andreae, M. O., and
650 Pöschl, U.: Cloud condensation nuclei in polluted air and biomass burning smoke near the mega-city
651 Guangzhou, China – Part 1: Size-resolved measurements and implications for the modeling of aerosol
652 particle hygroscopicity and CCN activity, *Atmos. Chem. Phys.*, 10, 3365–3383,
653 <https://doi.org/10.5194/acp-10-3365-2010>, 2010.

654 Saarnio, K., Frey, A., Niemi, J. V., Timonen, H., Rönkkö, T., Karjalainen, P., Vestenius, M., Teinilä, K.,
655 Pirjola, L., Niemelä, V., Keskinen, J., Häyrinen, A., and Hillamo, R.: Chemical composition and size of
656 particles in emissions of coal-fired power plant with flue gas desulphurization, *J. Aerosol Sci.*, 73, 14–26,
657 2014.

658 Schill, S. R., Collins, D. B., Lee, C., Morris, H. S., Novak, G. A., and Prather, K. A.: The impact of aerosol
659 particle mixing state on the hygroscopicity of sea spray aerosol. *ACS Central Science*, 1(3), 132-141,
660 2015

661 Sjögren, S., Gysel, M., Weingartner, E., Baltensperger, U., Cubison, M. J., Coe, H., Zardini, A. A., Marcolli,
662 C., Krieger, U. K., and Peter, T.: Hygroscopic growth and water uptake kinetics of two-phase aerosol
663 particles consisting of ammonium sulfate, adipic and humic acid mixtures, *J. Aerosol Sci.*, 38, 157–171,
664 doi: 10.1016/j.jaerosci.2006.11.005, 2007.

665 Suda, S. R., Petters, M. D., Matsunaga, A., Sullivan, R. C., Ziemann, P. J., and Kreidenweis, S. M.:
666 Hygroscopicity frequency distributions of secondary organic aerosols. *J. Geophys. Res.*, 117(D4), D04207,
667 2012

668 Svenningsson, B., Rissler, J., Swietlicki, E., Mircea, M., Bilde, M., Facchini, M. C., Decesari, S., Fuzzi, S.,
669 Zhou, J., Mønster, J., and Rosenørn, T.: Hygroscopic growth and critical supersaturations for mixed
670 aerosol particles of inorganic and organic compounds of atmospheric relevance, *Atmos. Chem. Phys.*, 6,
671 1937–1952, doi:10.5194/acp-6-1937-2006, 2006.

672 Sun, Y. L., Wang, Z. F., Du, W., Zhang, Q., Wang, Q. Q., Fu, P. Q., Pan, X. L., Li, J., Jayne, J., and
673 Worsnop, D. R.: Long-term real-time measurements of aerosol particle composition in Beijing, China:
674 Seasonal variations, meteorological effects, and source analysis, *Atmos. Chem. Phys.*, 15, 10149–10165,
675 doi: 10.5194/acp-15-10149-2015, 2015.

676 Sun, Y., Du, W., Fu, P., Wang, Q., Li, J., Ge, X., Zhang, Q., Zhu, C., Ren, L., Xu, W., Zhao, J., Han, T.,
677 Worsnop, D. R., and Wang, Z.: Primary and secondary aerosols in Beijing in winter: sources, variations
678 and processes, *Atmos. Chem. Phys.*, 16, 8309–8329, doi: 10.5194/acp-16-8309-2016, 2016.

679 Swietlicki, E., Hansson, H. C., HäMeri, K., Svenningsson, B., Massling, A., McFiggans, G., McCurry, P.
680 H., PetÄJÄ, T., Tunved, P., Gysel, M., Topping, D., Weingartner, E., Bal-tensperger, U., Rissler, J.,
681 Wiedensohler, A., and Kulmala, M.: Hygroscopic properties of submicrometer atmospheric aerosol
682 particles measured with H-TDMA instruments in various environments - a review, *Tellus B*, 60, 432–469,
683 doi: 10.1111/j.1600-0889.2008.00350.x, 2008.

684 Tan, H., Xu, H., Wan, Q., Li, F., Deng, X., Chan, P. W., Xia, D., and Yin, Y.: Design and application of an
685 unattended multifunctional H-TDMA system, *J. Atmos. Ocean. Tech.*, 30, 1136–1148, doi:
686 10.1175/JTECH-D-12-00129.1, 2013.

687 Turpin, B. J. and Lim, H. J.: Species contributions to PM_{2.5} mass concentrations: Revisiting common
688 assumptions for estimating organic mass, *Aerosol Sci. Tech.*, 35, 602–610, doi:
689 10.1080/02786820152051454, 2001.

690 Wang, J., Cubison, M. J., Aiken, A. C., Jimenez, J. L., and Collins, D. R.: The importance of aerosol mixing
691 state and size-resolved composition on CCN concentration and the variation of the importance with
692 atmospheric aging of aerosols, *Atmos. Chem. Phys.*, 10, 7267–7283, doi:10.5194/acp-10-7267-2010,
693 2010.

694 Wang, J., Zhang, Q., Chen, M.-D., Collier, S., Zhou, S., Ge, X., Xu, J., Shi, J., Xie, C., Hu, J., Ge, S., Sun,
695 Y., and Coe, H.: First chemical characterization of refractory black carbon aerosols and associated
696 coatings over the Tibetan Plateau (4730 m a.s.l), *Environ. Sci. Tech.*, 51, 14072,
697 doi:10.1021/acs.est.7b03973, 2017.

698 Wang, J. F., Liu, D. T., Ge, X. L., ~~Wu, Y. Z., Shen, F. Z., Chen, M. D., Zhao, J., Xie, C. H., Wang, Q. Q.,~~
699 ~~Xu, W. Q., Zhang, J., Hu, J. L., Allan, J., Joshi, R., Fu, P. Q., Coe, H., and Sun, Y. L.:~~ Characterization of
700 ~~black carbon containing fine 10 particles in Beijing during wintertime, *Atmos. Chem. Phys.*, 19, 447–458,~~
701 ~~doi: 10.5194/acp-19-447-2019, 2019.~~

702 Wang, Q., Zhao, J., Du, W., Ana, G., Wang, Z., Sun, L., Wang, Y., Zhang, F., Li, Z., Ye, X., and Sun, Y.:
703 Characterization of submicron aerosols at a suburban site in central China, *Atmos. Environ.*, 131, 115–
704 123, doi:10.1016/j.atmosenv.2016.01.054, 2016.

705 Wang, S. C. and Flagan, R. C.: Scanning Electrical Mobility Spectrometer, *Aerosol Sci. Tech.*, 13, 230–240,
706 1990.

707 Wang, Y., Zhang, F., Li, Z., Tan, H., Xu, H., Ren, J., Zhao, J., Du, W., and Sun, Y.: Enhanced
708 hydrophobicity and volatility of submicron aerosols under severe emission control conditions in Beijing,
709 *Atmos. Chem. Phys.*, 17, 5239–5251, doi: 10.5194/acp-17-5239-2017, 2017.

710 Wang Y., Li Z., Zhang Y., Du W., Zhang F., Tan H., Xu H., Fan T., Jin X., Fan X., Dong Z., Wang Q. and
711 Sun Y.: Characterization of aerosol hygroscopicity, mixing state, and CCN activity at a suburban site in
712 the central North China Plain, *Atmos. Chem. Phys.*, 18, 11739–11752, doi: 10.5194/acp-18-11739-2018,
713 2018a.

带格式的: 字体颜色: 黑色, 图案: 清除 (白色)

带格式的: 字体颜色: 黑色, 图案: 清除 (白色)

- 714 Wang, Y., Z. Wu, N. Ma, Y. Wu, L. Zeng, C. Zhao, and A. Wiedensohler: Statistical analysis and
715 parameterization of the hygroscopic growth of the sub-micrometer urban background aerosol in Beijing,
716 *Atmos. Environ.*, 175, 184-191, doi: 10.1016/j.atmosenv.2017.12.003, 2018b.
- 717 Wex, H., Petters, M. D., Carrico, C. M., Hallbauer, E., Massling, A., McMeeking, G. R., Poulain, L., Wu, Z.,
718 Kreidenweis, S. M., and Stratmann, F.: Towards closing the gap between hygroscopic growth and
719 activation for secondary organic aerosol: Part 1—Evidence from measurements, *Atmos. Chem. Phys.*, 9,
720 3987–3997, doi: 10.5194/acp-9-3987-2009, 2009
- 721 Wu, Z., Hu, M., Lin, P., Liu, S., Wehner, B., and Wiedensohler, A.: Particle number size distribution in the
722 urban atmosphere of Beijing, China, *Atmos. Environ.*, 42, 7967–7980, doi:
723 10.1016/j.atmosenv.2008.06.022, 2008.
- 724 Wu, Z. J., Poulain, L., Henning, S., Dieckmann, K., Birmili, W., Merkel, M., van Pinxteren, D., Spindler, G.,
725 Müller, K., Stratmann, F., Herrmann, H., and Wiedensohler, A.: Relating particle hygroscopicity and
726 CCN activity to chemical composition during the HCCT-2010 field campaign, *Atmos. Chem. Phys.*, 13,
727 7983–7996, doi: 10.5194/acp-13-7983-2013, 2013.
- 728 Wu, Z. J., Zheng, J., Shang, D. J., Du, Z. F., Wu, Y. S., Zeng, L. M., Wiedensohler, A., and Hu, M.: Particle
729 hygroscopicity and its link to chemical composition in the urban atmosphere of Beijing, China, during
730 summertime, *Atmos. Chem. Phys.*, 16, 1123–1138, doi: 10.5194/acp-16-1123-2016, 2016.
- 731 Xu, W. Q., Sun, Y. L., Chen, C., Du, W., Han, T. T., Wang, Q. Q., Fu, P. Q., Wang, Z. F., Zhao, X. J., Zhou,
732 L. B., Ji, D. S., Wang, P. C., and Worsnop, D. R.: Aerosol composition, oxidation properties, and sources
733 in Beijing: results from the 2014 Asia-Pacific Economic Cooperation summit study, *Atmos. Chem. Phys.*,
734 15, 13681–13698, doi: 10.5194/acp-15-13681-2015, 2015.
- 735 Ye, X., Tang, C., Yin, Z., Chen, J., Ma, Z., Kong, L., Yang, X., Gao, W., and Geng, F.: Hygroscopic growth
736 of urban aerosol particles during the 2009 Mirage-Shanghai Campaign, *Atmos. Environ.*, 64, 263–269,
737 doi: 10.1016/j.atmosenv.2012.09.064, 2013.

Zamora, M. L., Peng, J., Hu, M., Guo, S., Marrero-Ortiz, W., Shang, D., Zheng, J., Du, Z., Wu, Z., and Zhang, R.: Wintertime aerosol properties in Beijing, *Atmos. Chem. Phys.*, **19**, 14329–14338, <https://doi.org/10.5194/acp-19-14329-2019>, 2019.

Zardini, A. A., Sjogren, S., Marcolli, C., Krieger, U. K., Gysel, M., Weingartner, E., Baltensperger, U., and Peter, T.: A combined particle trap/HTDMA hygroscopicity study of mixed in-organic/organic aerosol particles, *Atmos. Chem. Phys.*, **8**, 5589–5601, doi:10.5194/acp-8-5589-2008, 2008

Zhang, F., Li, Y., Li, Z., Sun, L., Li, R., Zhao, C., Wang, P., Sun, Y., Liu, X., Li, J., Li, P., Ren, G., and Fan, T.: Aerosol hygroscopicity and cloud condensation nuclei activity during the AC3Exp campaign: Implications for cloud condensation nuclei parameterization, *Atmos. Chem. Phys.*, **14**, 13423–13437, doi: 10.5194/acp-14-13423-2014, 2014.

Zhang, F., Li, Z., Li, Y., Sun, Y., Wang, Z., Li, P., Sun, L., Wang, P., Cribb, M., Zhao, C., Fan, T., Yang, X., and Wang, Q.: Impacts of organic aerosols and its oxidation level on CCN activity from measurement at a suburban site in China, *Atmos. Chem. Phys.*, **16**, 5413–5425, doi: 10.5194/acp-16-5413-2016, 2016.

Zhang, F., Wang, Y., Peng, J., Ren, J., Zhang, R., Sun, Y., Collin, D., Yang, X., and Li, Z.: Uncertainty in predicting CCN activity of aged and primary aerosols, *J. Geophys. Res.-Atmos.*, **122**, 11723–11736, doi: 10.1002/2017JD027058, 2017.

Zhang, R., Khalizov, A. F., Pagels, J., Zhang, D., Xue, H., and McMurry, P. H.: Variability in morphology, hygroscopicity, and optical properties of soot aerosols during atmospheric processing, *PNAS*, **105**(30), 10291–10296, doi:10.1073/pnas.0804860105, 2008.

Zhang, R., Wang, G., Guo, S., Zamora, M. and Wang, Y.: Formation of urban fine particulate matter. *Chemical Reviews*, **115**(10), 3803-3855, 2015

~~Zhang, Q., Stanier, C. O., Canagaratna, M. R., Jayne, J. T., Worsnop, D. R., Pandis, S. N., & Jimenez, J. L.: Insights into the chemistry of new particle formation and growth events in Pittsburgh based on aerosol mass spectrometry, *Environ. Sci. Tech.*, **38**(18), 4797–4809, doi: 10.1021/es035417u, 2004.~~

Zhang, Y., Zhang, Q., Cheng, Y., Su, H., Kecorius, S., Wang, Z., Wu, Z., Hu, M., Zhu, T., Wiedensohler, A., and He, K.: Measuring the morphology and density of internally mixed black carbon with SP2 and

764 VTDMA: new insight into the absorption enhancement of black carbon in the atmosphere, *Atmos. Meas.*
765 *Tech.*, 9, 1833-1843, 2016.

766 Zhao, J., Du, W., Zhang, Y., Wang, Q., Chen, C., Xu, W., Han, T., Wang, Y., Fu, P., Wang, Z., Li, Z., and
767 Sun, Y.: Insights into aerosol chemistry during the 2015 China Victory Day parade: results from
768 simultaneous measurements at ground level and 260 m in Beijing, *Atmos. Chem. Phys.*, 17, 3215–3232,
769 doi: 10.5194/acp-17-3215-2017, 2017.